The Role of apoptosis in suicide gene therapy of glioblastoma

Shohana Afroz

This thesis is submitted in partial fulfilment of the requirements for the degree of Master in Biomedical Sciences

Department of Biomedicine

University of Bergen

Fall, 2021

Acknowledgements

Firstly, I would like to express my gratitude to my supervisor Jubayer Hossain and co-supervisor Professor. Hrvoje Miletic for welcoming me to the Miletic lab and allowed me to carry out the thesis on suicide gene therapy for glioblastoma treatment.

I would like to thank technical staff Halala Saed and Auera Castilho for their super support during my research work which helped a lot to run the experiments smoothly and always on time. Special thanks to Katharina Sarnow and Simon Storevik for their consistent support whenever required.

I am also grateful to Romi Roy Chowdhury, who helped me during the initial phase of the thesis and showed me the path to follow.

Ege Solel, this name will stand out throughout my research for her continued help and endless patience to answer my questions and put her hands on whenever necessary. I especially thank her for her contribution.

I would like to mention Aminur Rahman and Shahin Sarowar and thanks for providing support with the vast knowledge they possess in the field of Biomedicine.

I would also thank my family and friends for standing by me and encouraging me from start to finish.

Shohana Afroz,

Bergen, 2021

Summary

Glioblastoma (GBM) is the most malignant and one of the most frequent primary brain tumors. Current standard treatment regimen that includes maximal surgical resection with chemoradiotherapy translates into a dismal median survival of about 15 months after diagnosis. Thus, novel treatment strategies are needed to improve the poor prognosis of the GBM patients. Gene therapy is a promising strategy that may improve the survival of GBM patients. Suicide gene therapy by using HSV-TK and GCV as a prodrug has been extensively tested in the last couple of decades. Although preclinical studies and small-scale clinical trials showed positive results, large scale clinical trials failed to increase survival of the patients. Potential failures can be related to insufficient transgene delivery, poor cytotoxicity as well as lack of immune activation.

In this context, we have attempted to understand the cell death mechanism following this therapy. The mode of cell death induced by the treatment can shape the tumor microenvironment and thereby affect the potential efficacy. It can also directly impact the therapeutic outcome by either intensifying or curbing the resultant tumor-cell cytotoxicity. Hence, it is crucial to study and know more about the HSV-TK cell death mechanisms.
In this thesis, two widely used mouse glioma cell lines GL261 and CT2A along with a patient-derived glioblastoma cell line were employed to study the mechanism of cell death involved after HSV-TK-mediated suicide gene therapy. To explore the cell death mechanisms, we investigated the activation of cleaved caspase-3 after treatment since cleaved caspase-3 is a reliable marker for apoptosis. Cleavage of caspase-3 confirmed the initiation of apoptosis both in vitro and in vivo. Next, we investigated potential activation of the mitochondrial pathway and the death receptor pathway of apoptosis. We observed likely involvement of both, intrinsic and extrinsic apoptotic pathways.

In conclusion, our study demonstrates that apoptosis occurs in these glioma models after HSV-TK-mediated suicide gene therapy via likely simultaneous activation of both intrinsic and extrinsic pathways. In the future, it will be important to focus on the kinetics, interplay and relative significance of these two pathways in this context. It will also be important to investigate other cell death mechanisms apart from apoptosis which may play a significant role.

Table of Contents

Abbreviations

ACD Accidental cell death

Apaf-1 Apoptosis protease activating factor-1

APS Ammonium Persulfate

BBB Blood Brain Barrier

Bcl-2 B-cell lymphoma 2

bFGF Fibroblast Growth Factor-basic

BSA Bovine Serum Albumin

BSE Bystander Effect

CARD Caspase recruitment domain

DD Death domain

DED Death effector domains

DISC death-inducing signaling complex

DMEM Dulbecco's Modified Eagle's Medium

DMSO Dimethyl Sulfoxide

EGFR Epidermal growth factor receptor gene

FBS Fetal Bovine Serum

GBM Glioblastoma

GCV Ganciclovir

GCV-MP Ganciclovir Monophosphate

GCV-TP Ganciclovir Triphosphate

GJIC gap junction-mediated intracellular communication

GSC Glioblastoma cancer stem cell

HSV-TK Herpes Simplex Virus Thymidine Kinase

IDH1 Isocitrate Dehydrogenase 1

IL-8 Interleukin-8

kDa Kilodalton

LDS Lithium Dodecyl Sulfate

LOH Loss of Heterozygosity

MGMT Methylguanine DNA Methyltransferase

MOMP mitochondrial outer membrane permeability

NBM Neurobasal Medium

NCDD the Nomenclature Committee on Cell Death

PARP Poly (ADP-ribose) polymerase

PBS Phosphate buffer saline

PI3K Phosphatidyl inositol 3.4.5 biphosphate kinase

PTEN Phosphate and Tension Homolog on Chromosome 10

RCD Regulated cell death

RT Room Temperature

RTK Receptor Tyrosine Kinase

SDS Sodium Dodecyl Sulfate

SDS-PAGE Sodium Dodecyl Polyacrylamide Gel Electrophoresis

SGT Suicide Gene Therapy

TBS Tris Buffered Saline

TBS-T Tris Buffered Saline-Tween 20

TEMED Tetramethyl ethylenediamine

TK Thymidine Kinase

TMZ Temozolomide

WHO World Health Organization

WT Wild Type

1. Introduction

1.1 Cancer

Cancer is a group of diseases that are characterized by the uncontrolled growth of cells and subsequent spread to other parts of the body [1]. It is also considered a disease of the genome. Two broad classes of genes known as proto-oncogenes and tumor-suppressor genes, that exhibit dominant gain of function mutation and recessive loss of function mutation respectively, are crucial to cancer initiation [1]. Drs. Douglas Hanahan and Robert Weinberg sketched a framework outlining six hallmarks of cancer—self-sufficiency in growth signals, insensitivity to anti-growth signals, evading apoptosis, limitless replicative potential, sustained angiogenesis, tissue invasion and metastasis [2]. Gradually, the concept has been modified to include two more enabling characteristics such as genome instability and tumor-promoting inflammation. Later in 2011, the hallmarks of cancer were updated with the inclusion of reprogramming energy metabolism and avoiding immune destruction as emerging hallmarks [1, 3].

1.2 Brain Tumors

Brain tumors are characterized by abnormal cell growth within the brain. Some brain tumors are benign while others are malignant. Brain tumors developing within the brain are defined as primary tumors while tumors that spread from other parts of the body to the brain are known as secondary or metastatic brain tumors. The most common sources for secondary brain tumors are skin, colon, lungs and breast [4].

Primary brain tumors constitute only 2% of all primary cancers [5]. Gliomas, which are derived from glial cells or their precursor cells, are the most common type of primary brain tumors. According to the classification from World Health Organization (WHO), the main glial tumor groups include astrocytic tumors, oligodendroglial tumors, ependymal tumors, and neuronal and mixed neuronal-glial tumors. Astrocytomas are the most frequent gliomas which originate from astrocytes or their precursor cells. According to the WHO, gliomas are classified into 4 grades where 1 is the least aggressive and 4 is the most aggressive type. This grading is based on histopathological markers such as cellular density, nuclear atypia, mitosis, endothelial proliferation, and necrosis.

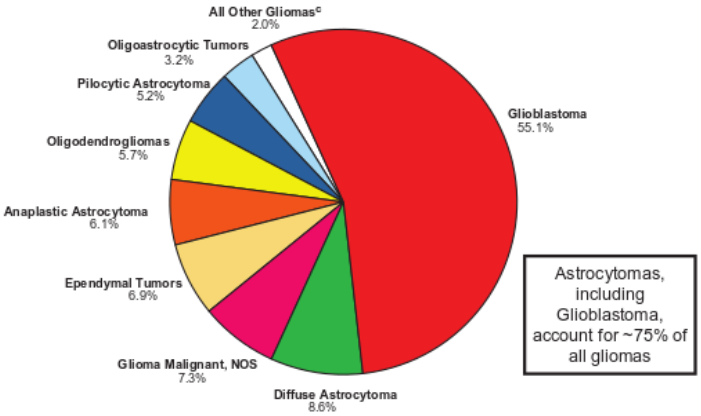

Figure 1 Distribution of primary central nervous system (CNS) gliomas by histological subtypes in USA 2008-2012 (n=97.910) Among all gliomas, astrocytomas including glioblastoma account for approximately 75% where glioblastoma is accounted as the majority of gliomas (55.1%). The figure was taken from [6].

1.3 Glioblastoma

Glioblastoma, the most frequent and most malignant type of glioma, is a WHO grade 4 glioma due to its aggressive nature [7]. Glioblastoma is the most common among all primary brain tumors in North America and Europe. In USA alone glioblastomas account for about 60 to 70% of all malignant gliomas [8]. It has a poor prognosis with approximately 15 months of median survival [9]. About 50% of the newly diagnosed patients with GBM each year die within one year and about 90% die within three years following diagnosis causing a substantial number of years loss in life than most other cancer types [10].

1.3.1 Etiology of GBM

No direct cause has been conclusively identified for GBM pathogenesis. However, there may be causative relationships between industrialization and the onset of GBM [11]. A higher incidence of GBM has been reported among the males who work in industries involved with rubber manufacturing, petroleum production, production of vinyl chloride, although none of these are established causes [12] [7]. Exposure to ionizing radiation is one of the physical causes that increase the chance of developing GBM. Certain metals and electromagnetic fields are also being studied and considered to be involved in the development of glioma [12]. GBM can also be promoted during a genetic disease such as tuberous sclerosis, Turcot syndrome, Multiple

Endocrine Neoplasia (MEN) type IIA and Neurofibromatosis type I (NF1). A relationship between brain injuries and onset of glioblastoma has also been reported as a potential etiologic trigger for GBM [12]. In addition, some viruses can be etiologic agents for gliomagenesis. The most prominent example is human cytomegalovirus (HCMV) which is believed to be among the etiologic agents for glioma development, however this is still heavily debated.

1.3.2 Molecular pathogenesis

GBMs are divided into primary and secondary GBM. Primary GBM, which develop de novo typically in older patients above the age of 50, is the most common form with more than 90% of cases. Secondary GBMs develop from low-grade astrocytoma in younger patients and have a mutation in the IDH 1 or IDH 2 gene. Primary GBM, by definition, are IDH wild-type GBM [13].

GBM growth is promoted by deregulation of the G1/S checkpoint of the cell cycle and genetic disturbances such as loss of chromosome10q, gain of chromosome 7 and EGFR amplification [12]. Mutations in PTEN, TP16, TP53, PARK2, PTPRD and NF1 are also common in GBM pathogenesis [12, 14] Epidermal growth factor receptor gene (EGFR) amplification occurs in about 40% of primary GBM and is rarely found in secondary GBMs. PTEN gene mutations are present in 15-40% of primary GBMs while they are rarely found in secondary GBM. In contrast, TP53 mutations are more common in secondary than primary GBMs (65%*vs* 28%). Homozygous deletion of the $p16^{INK4a}$ gene, CDK4 amplification, and loss of RB are found in about 50% of primary GBM and 40% of in secondary GBM. Based on expression profiles of different types of GBMs, several molecular subclasses have been proposed such as classical, mesenchymal, proneural and neural subtypes [15]. Classical GBM are characterized by EGFR amplification and loss of chromosome 10, but they lack mutations in IDH1, TP53 or NF1. The mesenchymal subtype is associated with NF1 and PTEN mutations. The neural subtype is defined by normal brain tissue gene expression profile and astrocytic/oligodendrocytic cell markers. The proneural subtype is defined by focal amplification of PDGFRA as well as TP53 and IDH1 mutations and thus consists mostly of secondary GBM. Histologically, primary and secondary forms of GBM can be indistinguishable but vary in genetic and epigenetic profiles. Proneural gene expression pattern is found in most of GBM with IDH1 mutations which makes IDH1 a reliable molecular diagnostic criterion of secondary GBM [15]. Secondary GBM is mostly a proneural subtype

and genetically more homogenous group when it comes to IDH1 mutation compared to primary GBM.

1.4 Treatment

GBM requires a multimodal treatment approach. The standard approach in managing GBM includes consideration of maximum surgical resection followed by concurrent radiation and chemotherapy. As GBM cells invade into the surrounding healthy tissue, it is not possible to achieve complete resection. Extent of resection has an impact on survival as well as quality of life of the patients [16]. Radiation has been historically used as a reliable treatment modality for GBM. Radiation triggers DNA damage causing the cells to undergo apoptosis and kill the bulk of tumor mass [17] [18].

Temozolomide (TMZ), an oral alkylating drug, is the standard chemotherapeutic agent for GBM treatment [19]. TMZ methylates the purine bases of DNA at N7 and O6 position positions of guanine (N7 MeG-70% and MeG-6%) and N3 position of adenine. Methylated O6 position of guanine lesion causes DNA double-strand break (DSB) that leads to cell cycle arrest and apoptosis. However, DNA base excision repair (BER) recovers the lesions at N7-MeG and N3-MeA positions [20]. O^6-methylguanine-DNA methyltransferase (MGMT), a DNA repair enzyme, is important in the DNA-damage response. TMZ treatment effectiveness has a relationship with MGMT activity where methylated MGMT cannot protect tumor cells from DNA damage and leads DNA repair mechanisms to fail [21] [22].

Development of novel treatment strategies for GBM has been hindered by the complex nature of the disease. Multiple gene mutations, chromosomal aberrations and gene fusions underpin the complexity of GBM [23]. Most importantly tumor cells undergo clonal evolution during tumor development which leads to tumor heterogeneity [24]. In addition, the blood-brain-barrier (BBB) stands out as a structural obstacle. Many potential drugs cannot cross BBB.

Gene therapy, in this context, has been a promising experimental treatment modality for GBM treatment for many years which can potentially overcome some of these challenges.

1.5 Gene therapy

Gene therapy is an experimental approach to treat a disease by transferring genetic material into target cells. Gene therapies for GBM include delivery of suicide genes, cytokine genes, tumor-suppressor genes and oncolytic viruses [10] (Figure 2). In gene therapy, viruses are frequently chosen as gene-delivery vehicles or vectors because they are highly efficient at inserting nucleic acids into specific cell types [25]. Neural or mesenchymal stem cells can also provide alternative delivery methods as they can spread within tumor tissues and possess the ability to migrate to distant tumor areas [26].

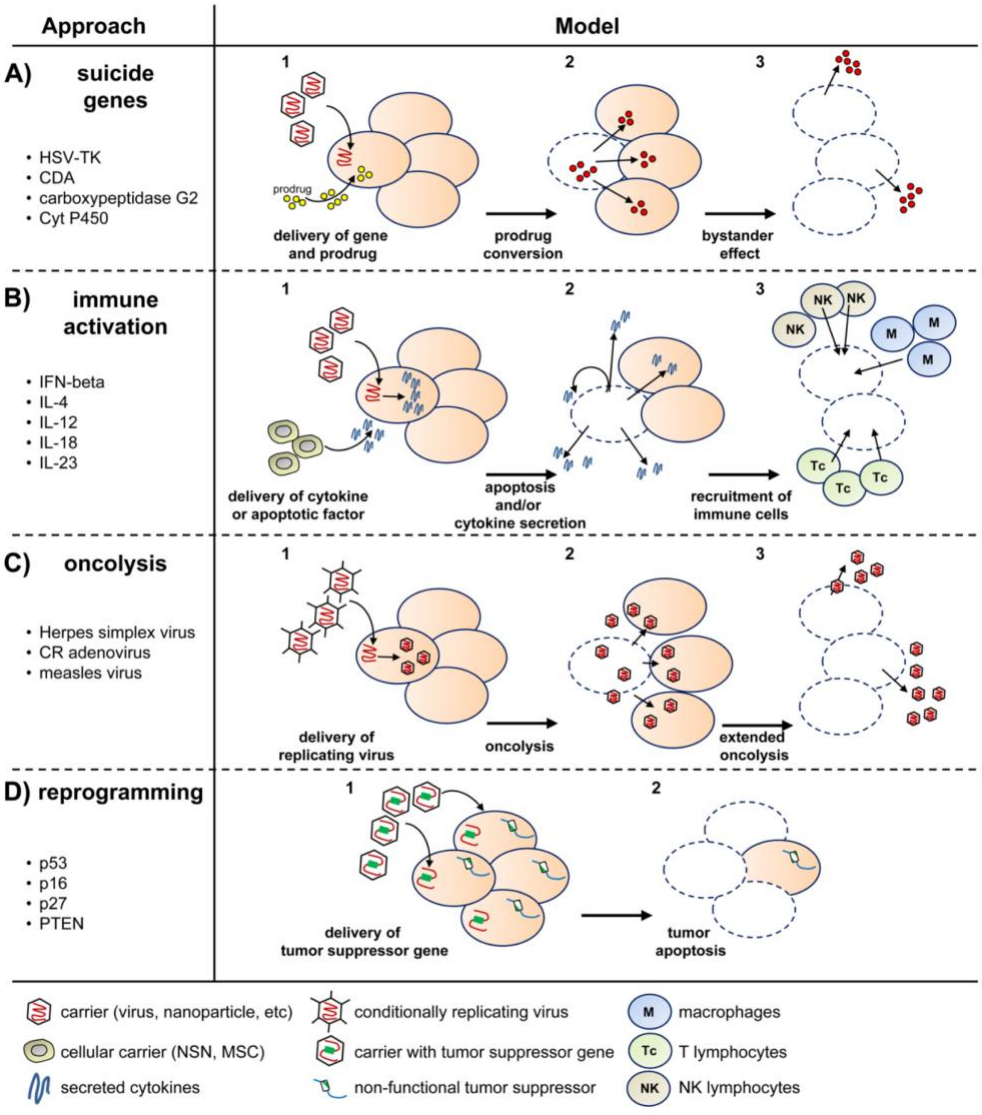

Figure 2 Major gene therapy approaches of GBM [10].

1.5.1 Suicide gene therapy

At present, suicide gene therapy (SGT) is the most widely used experimental gene therapy for treating malignant glioma. The concept of this strategy is to introduce a gene (often of viral or bacterial origin) into tumor cells which is capable of converting a non-toxic compound, known as prodrug, into a deadly drug that can induce tumor cell death [27]. Among the various types of suicide gene therapy systems, Herpes Simplex Virus Thymidine Kinase (HSV-TK) and Cytosine Deaminase 5-fluorocytosine (CD) are the most common suicide genes [26]. In this thesis, we will focus on HSV-TK-based suicide gene therapy system with ganciclovir (GCV) as prodrug.

While several prodrugs can be used in the HSV-TK-based suicide gene therapy system, ganciclovir (GCV) is the most widely used prodrug. The expression of HSV-TK leads to catalysis of GCV into ganciclovir monophosphate (GCV-MP). Further phosphorylation of GCV-MP by cellular kinases produce ganciclovir triphosphate (GCV-TP). GCV-TP functions as a nucleoside analogue and becomes incorporated into DNA of actively dividing cells ultimately causing cell cycle arrest and apoptosis[28]. HSV-TK detects GCV more efficiently than cellular TK and as a result, the toxicity does not affect normal brain cells [29].

There are two major types of viral vectors used for treating GBMs. The first type is replication-deficient viruses. The second type is replication-competent viral vectors. The replication-competent viruses also include oncolytic viruses which have a lytic cycle and thus kill tumor cells selectively [26]. Adenoviral, retroviral, lentiviral and non-viral vectors have been the most popular delivery systems. Lentiviral vectors are very promising candidates due to their ability of genome integration into both dividing and non-dividing cells [29].

A recombinant version of HSV-TK, termed TK.007 has been engineered which shows superior activity compared to the wild type HSV-TK [30]. In this thesis we have used HSV-TK.007.

1.5.2 Bystander effect

In HSV-TK/GCV suicide gene therapy, the metabolized GCV can be transferred from transduced to untransduced neighbouring tumor cells which thus are exposed to GCV-mediated cytotoxicity even if they lack HSV-TK expression. This phenomenon is termed as the “bystander effect” (BSE) which greatly increases the efficacy of the therapy. Gene transfer in

SGT is a limiting factor; hence BSE is essential to promote therapeutic efficacy. For example, less than 10% transduction of tumor cells could still be adequate to eradicate the entire cancer cell population [31]. This principle explains that only a small portion of tumor cells need to express HSV-TK to achieve extensive killing after GCV administration [31].

There are a few possible mechanisms for the bystander effect. The most prominent one is gap junction-mediated intracellular communication (GJIC; Figure 3). Gap junctions are a cluster of channels made of membrane proteins. These junctions allow intracellular communication between neighboring cells by diffusion of ions and molecules. Six connexin proteins build up a connexon through oligomerization at the cell surface which ensures for junction- mediated intracellular communication [32]. The primary mechanism of BSE in vitro has been attributed to gap junction protein Connexin-43 but the heterogeneous expression of connexins might impact the efficiency of HSV-TK/GCV therapy [33].

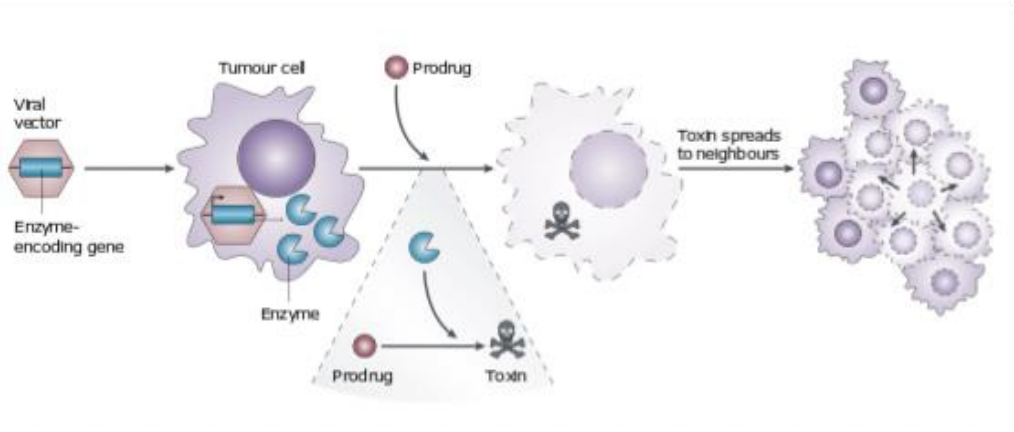

Figure 3 BSE is defined by spread of the toxic drug through gap junction to neighbouring, untransduced cells. Figure adapted from [34].

1.6 Cell death

Cell death is a vital process that occurs during the normal development of both vertebrates and invertebrates. Everyday cell death occurs in billions of cells in the human body to maintain tissue homeostasis, to support recovery from an acute injury, to deal with infection, and to regulate immunity [35].

Based on morphological alterations, cell death is historically classified into three different forms. Type I cell death or apoptosis is characterized by nuclear fragmentation, cytoplasmic

shrinkage, chromatin condensation and plasma membrane blebbing. This process generates apoptotic bodies which are eliminated through phagocytosis by phagocytic cells such as macrophages [36].

Type II cell death or autophagy is a cellular self-eating process to anomalous proteins, and damaged cytoplasmic organelles [37] . The type III cell death or necrosis does not contain any well-defined features from type I or II cell death. It is an unregulated cell death characterized by cell swelling and rupture of the plasma membrane followed by cytoplasmic leakage into surrounding tissues [38] [39].

In 2005, the Nomenclature Committee on Cell Death (NCDD) upgraded this classification and fundamentally divided cell death into two forms: accidental cell death (ACD) and regulated cell death (RCD) [38]. ACD is instantaneous and catastrophic form of cell death triggered by unexpected injuries and insults, including physical (e.g., high pressures and temperatures), chemical (potent detergents or extreme variations in pH), or mechanical (e.g., shear forces) stimuli. In response to extracellular or intracellular stresses, RCD can occur as part of physiologic programs, also called programmed cell death. RCD is tightly involved in signaling cascades and has a set of defined executor molecules. Regulated cell death has a unique biochemical, functional, and immunological outcome [40].

Regulated cell death is classified into multiple subtypes based on its molecular characteristic including apoptosis, mitochondrial permeability transition (MPT)-driven necrosis, necroptosis, pyroptosis, ferroptosis, parthanatos, and entosis [38].

1.7 Apoptosis

Apoptosis is a highly preserved and controlled form of programmed cell death that exhibits an orderly and efficient removal of damaged cells without disrupting the overall homeostasis of the tissue. Apoptosis occurs both during development and aging. In apoptosis, dying cells show marked morphological changes such as cell shrinkage and condensation, cytoskeleton collapse and disassembly of the nuclear envelope. Furthermore, nuclear chromatin condenses, and breaks up into fragments. At the later stage of apoptosis, the cell surface often blebs and forms apoptotic bodies. Before the completion of apoptosis, cells split their content. Macrophages and other neighboring cells rapidly engulf them without eliciting inflammation. [41] [42] [43].

Apoptotic cells also show biochemical changes. In normal cells, phospholipid phosphatidylserine is normally located in the inner leaflet of the lipid bilayer of the plasma membrane. But in apoptotic cells, phospholipid phosphatidylserine is found in the outer leaflet of the plasma membrane. It serves as an "eat me" signal by sending signals to neighboring cells and macrophages to phagocytose the dying cell. It also inhibits the production of inflammation-inducing signal proteins from the phagocytic cell to block inflammation [32].

1.7.1 Caspases

Caspases are important in the central machinery responsible for cell death and inflammation in all animals. Currently, 14 distinct mammalian caspases have been identified which belong to a family of evolutionarily conserved cysteine-dependent endoproteases that cleave target proteins at specific aspartic acids residues [44]. Caspases are synthesized in the cells as inactive precursors called procaspases. Procaspases are activated by proteolytic cleavage. Procaspases have a highly diverse structure on their N-terminal region that involves caspase activation. After proteolytic cleavage, procaspases are split into two sub-units, a large and a small subunit respectively, to produce a heterodimer. Two heterodimers then form an enzymatic active heterotetramer that cleaves other procaspases to activate them. Among the 12 caspases found in humans [45], caspase-2, -3, -6, -7, -8, -9, -10 are involved in apoptotic cell death [46]. In contrast, caspase-1, -4, -5, -11 are involved in other forms of cell death including pyroptosis, which often is pro-inflammatory [47, 48]. Based on amino acid sequences homology, the apoptotic caspases are divided into two types: initiator, and executioner caspases [49]. Caspase-2, -8, -9, and10 are member of the group of initiator caspases that can initiate apoptosis and are responsible for activating the executioner caspases-3, -6, and -7 [44] [32].

The initiator procaspases have a caspase recruitment domain (CARD; caspases-1, -2, -4, -5, -9, -11) or death effector domains (DED; caspases-8, -10) at the N-terminal end. These two domains are member of a death domain family which are involved in recruitment, activation, and downstream caspase-cascade regulation through protein-protein interactions. When cells receive an apoptotic stimulus, the initiator procaspase assembles into the activation complex with the CARD domain that brings them into proximity. The initiator caspases then cleave each other to activate them irreversibly. In contrast, the activation of executioner caspases depends on the initiator caspases due to the lack of extended amino-terminal prodomain [47].

The activated effector caspases have a broad spectrum of cellular targets to induce apoptosis. Some of the cellular targets for the activated effector caspases are cellular structural components (such as actin and nuclear lamin), regulatory proteins (such as DNA-dependent protein kinase), inhibitors of deoxyribonuclease, and other proapoptotic proteins and caspases. Furthermore, they also inhibit the action of DFF40 or CAD (caspase-activated deoxyribonuclease) to degrade the chromosomes into nucleosomal fragments during apoptosis [44]. Based on the route of the apoptotic pathway, apoptosis can be divided into two groups, intrinsic and extrinsic pathways.

1.7.2 Intrinsic apoptosis

The intrinsic apoptotic pathway is a mitochondria-dependent apoptotic pathway. It depends on the release of mitochondrial proteins into the cytosol which is initiated by intracellular signals in response to different stress conditions, including irradiation, treatment with chemotherapeutic agents etc. [50]. Usually, internal stimuli such as irreparable DNA damage, lack of nutrients, hypoxia, extracellular survival signals, extremely high concentrations of cytosolic Ca^{+}, and severe oxidative stress trigger the intrinsic pathway. The B-cell lymphoma 2 (Bcl-2) family proteins play a critical role in this pathway by [42] promoting mitochondrial outer membrane permeability (MOMP). This event releases proteins that are normally enclosed in the inter-membrane space of the mitochondria into the cytosol [51] . Cytochrome c is one of the mitochondrial proteins that play a crucial role in activating the mitochondrial-dependent death in the cytosol. Cytochrome-c binds to the procaspase activating adaptor protein called apoptosis protease activating factor-1 (Apaf-1) in the cytosol and induces the oligomerization of Apaf 1 into a wheel-like heptamer called an apoptosome. Apoptosome is composed of initiator pro-caspase-9 with its caspase recruitment domain (CARD) and is activated by proximity. Finally, the activated caspase-9 molecules then activate downstream executor caspases-3, -6, and -7 to activate them and induce cleavage of cellular substrates leading to apoptotic cell death [42] [52] [53] [32] (Figure 4).

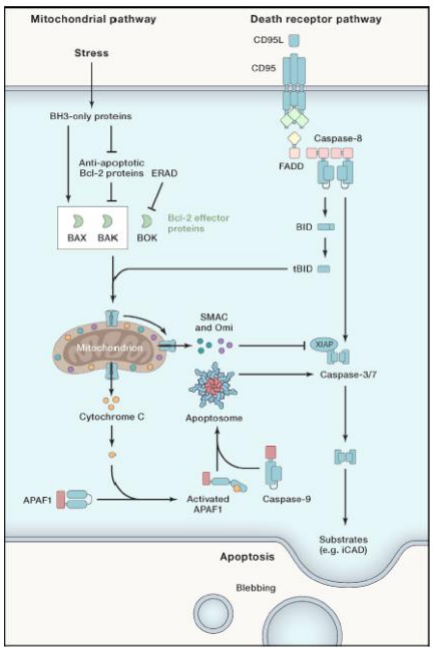

Figure 4 Schematic representation of two main apoptotic pathways [54].

1.7.3 B-cell lymphoma-2 (Bcl-2) family proteins

The Bcl-2 family consists of three different types of proteins: (1) anti-apoptotic Bcl-2 family proteins (2) pro-apoptotic BH123 proteins and (3) pro-apoptotic BH3-only proteins. As a result, the Bcl-2 family proteins regulate both pro-apoptotic and anti-apoptotic intrinsic pathways by controlling MOMP and thus serve as an apoptotic switch [42]. All members of the Bcl-2 protein family have sequence homology within a conserved region known as BCL-2 homology (BH) domains [55]. The anti-apoptotic Bcl-2 family proteins share three to four distinctive BH domains (numbered BH1 to BH4). The pro-apoptotic BH123 protein group has three BH-domains (BH1, BH2 and BH3) but the BH3-only protein group has only the BH3 domain. The BH1 and BH2 domain of the Bcl-2 family bind with pro-apoptotic proteins to initiate dimerization. The BH3 domain is necessary for the interaction between pro-apoptotic and anti-apoptotic proteins. Overall, whether a cell lives or undergoes apoptosis mainly depends on the balance between the interaction of the pro-apoptotic and the anti-apoptotic proteins [32] [42].
Anti-apoptotic multidomain members of the Bcl-2 protein family includes Bcl-2 (B-cell lymphoma 2) itself, B-cell lymphoma-extra-large (Bcl-xL), B-cell lymphoma-w (Bcl-W), BCL-2-related protein A1, myeloid cell leukemia-1(Mcl-1), and B-cell lymphoma- B (Bcl-B) located on the cytosolic surface of the mitochondrial outer membrane, the ER and the nuclear envelope. Their main role is to preserve the membrane integrity by engaging in direct inhibitory

interactions with Bak and Bax to prevent release of mitochondrial proteins and Ca2+ from endoplasmic reticulum (ER) [42].

BAK and Bax are the main pro-apoptotic BH123 proteins in the Bcl-2 family. Bak is an integral membrane protein located in the mitochondrial outer membrane and the outer surface of the endoplasmic reticulum in the absence of apoptotic signal. Bax is a cytosolic protein that translocate to the mitochondria after activation [32].

In response to apoptotic stimuli, the BH3- only proteins are activated. The major proteins in this group are Bid (BH3 interacting-domain death agonist), Bim (Bcl-2-like protein 11), Bad (Bcl-2-associated death promoter), Puma (p53 upregulated modulator of apoptosis), Noxa, BMF, HRK and BIK. These BH3 only proteins bind to anti- apoptotic proteins to inhibit their activity, thereby allowing the aggregation and oligomerization of BAK and Bax to elicit the permeabilization of the outer mitochondrial membrane (OMM) [32].

1.7.4 Extrinsic apoptotic pathway

The death receptor (or extrinsic) pathway of apoptosis is initiated by the binding of extracellular signal protein to the cell surface-exposed death receptor (Figure 4). The death receptors are transmembrane proteins that belong to the superfamily of tumor necrosis factor receptors (TNFR), containing an extracellular ligand-binding domain, a single transmembrane domain, and an intracellular death domain. The receptors are homotrimers and the intracellular death domain is crucial for the activation of the apoptotic program. The ligands are also homotrimers which can be a group of complementary cytokines that belong to the TNF protein family that bind with their corresponding receptors. Some of the most studied death receptor-ligand signaling systems are Tumor necrosis factor receptor 1-Tumor necrosis factor α ligand (TNFR1-TNFα), Fas receptor- Fas ligand (FAS (CD95, APO-1)-FasL), Tumor necrosis factor-related apoptosis-inducing ligand receptor 1- Tumor necrosis factor-related apoptosis-inducing ligand (TRAILR1 (DR4)-TRAIL), Tumor necrosis factor-related apoptosis-inducing ligand receptor 2- Tumor necrosis factor-related apoptosis-inducing ligand (TRAILR2 (DR5)-TRAIL) [42].

Death receptors are activated upon ligand binding. The intracellular region of the death receptors, upon ligand binding, recruit different intracellular adaptor proteins (for example, Fas-associated protein with death domain or FADD, TNF receptor-associated protein with death

domain or TRADD etc.), which in turn recruit initiator procaspases (procaspase-8, procaspase-10 or both) [56]. The association of the adaptor molecule and the receptor is mediated by the homotypic interaction of death domain (DD) of the receptors with the DD of the adaptor molecules. Additional protein-protein interaction modules, such as death effector domains (DEDs) may also be observed. Overall, the association of ligand-induced receptor and adaptor form the death-inducing signaling complex (DISC) at the plasma membrane. Death-inducing signaling complex then initiates apoptosis by increasing the local concentration of pro-caspase that induces proximity resulting in auto-activation [57] [58]. The activated initiator caspase cleaves downstream effector caspase-3, -6, -7, which leads to the cleavage of essential substrates for cell viability, inducing cell death [59].

Not all cells can produce a sufficient amount of cleaved caspase-8 as well as can't activate downstream caspases to complete apoptosis. In this case, a mitochondrial amplification step is necessary to initiate death receptor apoptosis that is induced by active (cleaved) caspase-8. In this specific pathway, caspase-8 cleaves the BH3-only proapoptotic cytosolic protein Bid (BH3-interacting-domain death agonist) and generates the activated fragment t-Bid [59]. t-Bid then translocates to mitochondria and oligomerizes with the pro-apoptotic Bcl-2 family members Bax and Bak to induce mitochondrial outer membrane permeability (MOMP). As a result, cytochrome c is released from mitochondria into the cytosol and initiates the same cascade as in the intrinsic pathway. Released cytochrome c binds with apaf-1 and oligomerizes into the apoptosome. This protein complex binds with the initiator caspase-9 and activates them. Activated caspase-9 cleaves executioner caspases-3 and -7 to initiate the execution of apoptosis [59].

2. Aims

The present thesis aims to explore the mechanism of cell death a selected panel of glioma cell lines after HSV-TK/GCV treatment. Briefly, our objectives were as follows:

- To investigate the potential activation of apoptosis after HSV-TK/GCV treatment
- To investigate the potential activation of Intrinsic apoptotic pathway after HSV-TK/GCV treatment
- To investigate the potential activation of Extrinsic pathway after HSV-TK/GCV treatment

3. Materials and Methods

3.1 Cell culture

3.1.1 Media Preparation

Dulbecco's Modified Eagle's Medium (DMEM):

DMEM (Sigma-Aldrich Inc., St. Louis, MO, USA) was supplemented with 10% heat-inactivated Fetal bovine serum (FBS) (10270-106, Gibco, Life Technologies Limited, Brazil), 2% (v/v) L-glutamine (BioWhittaker), 2% (v/v) Penicillin-Streptomycin (BioWhittaker, Verviers, Belgium), 0.02% Plasmocin (Invitrogen, Toulouse, France), 3.2% non-essential amino acids (NEAA) (13-114E, Lonza, Walkersville MD USA). DMEM in this section includes all the supplements that will be treated as complete DMEM throughout the thesis.

Neurobasal Medium (NBM):

NBM was supplemented with 1% (v/v) Penicilin- Streptomycin, 1% (v/v) L-Glutamine, 2% (v/v) B27-A Supplement (50X) (1258-010, 2313378, GibcoTM,Thermo Fisher Scientific, 0.1% Heparin LEO 5000 IE/ml (Vitusapotek), 20 ng/ml Fibroblast Growth Factor-basic (bFGF) (100-18B, PeproTech®,Germany). NBM in this section includes all the supplements that will be treated as complete NBM throughout the thesis.

Cell freezing media: Complete DMEM was supplemented with 10% (v/v) Dimethyl sulfoxide (DMSO) (Sigma-Aldrich, Steinheim, Germany) and 10% (v/v) FBS.

3.1.2 Drug Preparation

GCV (G2536, Sigma-Aldrich, USA) was dissolved in complete DMEM to a final concentration of 3 mM and aliquoted in 500 µl microcentrifuge tubes (Eppendorf, Germany). Aliquoted GCV was stored at -20°C.

Dulbecco's Modified Eagle's Medium (DMEM) with Ganciclovir (GCV): 3 mM GCV was diluted in complete DMEM to make final concentration of 20 µM.

Neurobasal Medium (NBM) with Ganciclovir (GCV): 3 mM GCV was diluted in complete NBM to make final concentration of 20 µM.

Raptinal (SML1745, Sigma-Aldrich) was dissolved in DMSO to a final concentration of 25 mM and kept at 4 °C. Further dilution was done just prior to experiment to reach 10 μM.

3.1.3 Cell Lines

P3: Patient-derived GBM cell line P3 has been collected from a surgical GBM resection undertaken at the Haukeland University Hospital, Norway and grown in Neurobasal medium [60].

P3.TK.GFP: Previously P3 cells were transduced with lentiviral HSV-Tk.007 at the laboratory Prof. Hrvoje Miletic. This cell line is designated as P3.TK.GFP throughout the thesis. [61].

CT2A: CT2A is a mouse glioma cell line derived from a sub-cutaneous, non-metastatic murine glioma (astrocytoma) [62].

CT2A.TK.GFP: Previously CT2A-TK cells were transduced with lentiviral HSV-Tk. 007 at the laboratory Prof. Hrvoje Miletic. This cell line is designated as CT2A.TK.GFP throughout the thesis [61].

GL261: In vivo GBM models based on the mouse glioma 261 (GL261) cell line are the most frequently used immunocompetent models in experimental glioblastoma therapy [63].

GL261.TK.GFP: Previously GL261cells were transduced with lentiviral HSV-Tk. 007 at the laboratory Prof. Hrvoje Miletic. This cell line is designated as GL261.TK.GFP throughout the thesis [61].

3.1.4 Sub-culturing and Passaging

Cells were incubated in the humidified incubator (Thermo Forma, Steri-Cycle CO_2 Incubator, 301310-634, Ohio, USA) at 37 °C with 5% CO2 and passage them when they reached 70-90% confluency. 1X Dulbecco's Phosphate buffer saline (PBS) was used as wash buffer. 10X PBS (D1408, Sigma Aldrich, St Louis, Missouri, USA) dissolved in MilliQ-H_2O (QGARD00R1, Millipore, France) to prepare 1X PBS. The cells were centrifuged at 1250 rpm by using an Eppendorf Centrifuge (5810 R Sigma-Aldrich, Steinheim, Germany) and routinely monitored by using a Nikon Eclipse TS100 (Nikon Corporation, Tokyo, Japan) inverted microscope. A sterile laminar hood was used to do all cell culture work.

Gl261 WT, GL261.TK.GFP and CT2A WT, CT2A.TK.GFP

When cells reached 70-90% confluency, the old medium from the culture flask was removed and the cells were washed with 1X PBS. 2 ml of trypsin-versene mixture (Cat no. 17-161E, Lanza, USA) was added for 5 minutes to detach the cells from each other as well as from the culture flask by breaking down the adhesive proteins. 8 ml complete DMEM medium was added to neutralize the trypsin activity and cells were then transferred to a 15 ml falcon tube. The cells were centrifuged at 1250 rpm for 5 minutes, medium was removed, and cells were resuspended with fresh medium. Resuspended cells were then added to fresh flasks or used for counting.

P3 WT and P3.TK.GFP

The cells were detached from the flask surface by a cell scraper and collected into 15 ml falcon tubes. These tubes were centrifuged at 1250 rpm for 5 minutes and old medium was removed. Cells were resuspended with 1x PBS for washing and centrifuged at 1250 rpm for 5 minutes. PBS was removed and the cell pellet was resuspended in complete NBM. The cells were then dissociated into single cells by pipetting up and down.

3.1.5 Cell counting and determination of viability

Cell counting is necessary to obtain a definite number of cells for in vitro experiments. A hemocytometer (8100203, Neubauer, Hirschmann Laborgeräte GmbH & Co, Eberstadt, Germany) covered with cover glass (Menzel-Gläser, Thermo Scientific) was used to count the cells by using Trypan blue which can differentiate live and dead cells. To count the cells, 20 µl of cell suspension was mixed with 80 µl of trypan blue (Life Technologies, OR, US). From this mixture, 10 µl of single cell/Trypan blue dye suspension was loaded to each chamber of hemocytometer and covered with the glass cover.

The hemocytometer area is splited into 9 squares of 1mm x 1mm in size just like a tic-tac-toe grid. Each square has dept of 0.1 mm. The Four squares in the corner (marked in green in Figure 5) are further divided into 4 x 4 grids which we have used to count the cells. The formula for the cell concentration is

Number of cells/ml = (Average cell count x Dilution Factor x 10^4)

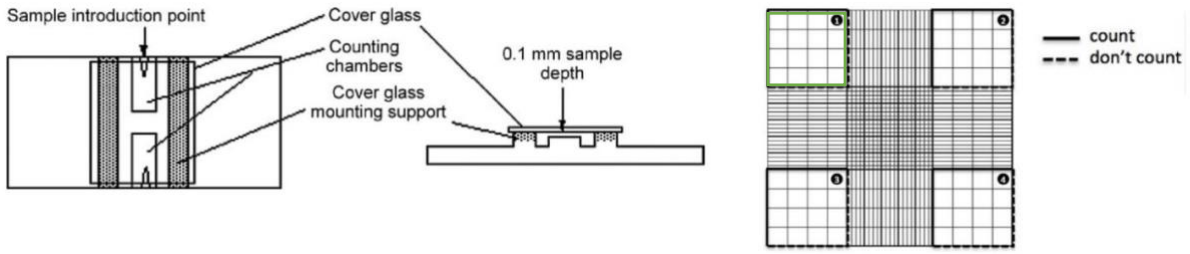

Figure 5 Hematocytometer. Left: Top view of Hematocytometer Right: 4 big squares chambers of Hematocytometer. Cell presentation with dotted lines were not counted. Figure adapted from [64].

3.1.6 Thawing of cells

Required Cell culture medium for corresponding cell line was pre-warmed in a water bath at 37 ˚C. T75 culture flasks were labelled and prepared with 10 ml cell culture medium. The cryo-preserved cells were taken out from -80 °C and placing them into 37 °C water bath for 2 minutes. Before transferring to the laminar air hood, the vials were wiped with 70% alcohol. Immediately, the cell suspension was transferred into a 15 ml falcon tube which was prepared with 10 ml pre-warmed 1X PBS and centrifuged at 1250 rpm for 5 minutes. The supernatant was discarded after centrifugation and the cell pellets were resuspended into the required media. The culture flask was placed inside the incubator at 37 °C. The medium was replaced with a fresh medium after overnight incubation and incubated until they reached about 80% confluency.

3.1.7 Freezing of cells

For long term storage, cells need to be frozen down in liquid nitrogen. After 5-10 passages when cells reached 70-90% confluency, they were washed with 1X PBS, trypsinized, transferred to a 15 ml falcon tube and centrifuged at 1250 rpm for 5 minutes. The supernatant was discarded, and the cell pellets were resuspended into freezing medium. The cells in freezing medium were pipetted into 1.0 ml cryotubes (377224, Thermo Fisher Scientific, Massachusetts, USA) and placed in a Mr. FrostyTM Freezing Container (C1562, Sigma-Aldrich, Steinheim, Germany). The cells were kept at -80 °C for 24 hours to provide a gradient transition of temperature change. After 24 hours, cryotubes were transferred from -80 °C freezer to a nitrogen tank for long-term storage.

3.2 Drug Treatments

3.2.1 Ganciclovir treatment

Gl261.TK.GFP, CT2A.TK.GFP and P3.TK.GFP monolayer cells were seeded at a density of $1.5x10^6$ into the T25 culture flask (156367, Thermo Scientific, Denmark). After overnight incubation, cells were treated with 20 μM GCV and incubate at 37 °C incubator. Gl261.TK.GFP and CT2A.TK.GFP cells pellets were collected after 24 hours and 48 hours of GCV treatment. After 24 hours, 48 hours and 72 hours of treatment P3.TK.GFP cells pellets were collected. Collected cell pellets were washed with 1X PBS and lysed with ice cold M-PER Mammalian Protein Extraction Reagent (78503, Thermo Fisher Scientific, Waltham, Massachusetts, USA) with 1% phosphatase inhibitor (04906845001, Roche, Indianapolis, USA) and 1% protease inhibitor cocktail (04693124001, Roche, Manheim, Germany). Resuspended cell pellets were incubated on ice for 30 minutes and vortexed every 10 minutes for proper lysis. After 30 minutes, cell lysate was spun down at 14000 rpm for 10 minutes at 4 °C by using a centrifuge (Centrifuge 5424 R, Eppendorf, Hamburg, Germany) to separate cellular debris from the protein lysate. Finally, the lysates were transferred to new pre- chilled 1.5 ml microcentrifuge tubes and stored at -80 ˚C for future use.

3.2.2 Cytochrome c release

The presence of cytochrome c was detected by immunoblotting against the cytochrome c antibody. 5×10^6 were seeded in T125 culture flask and incubate at 37 °C incubator. After overnight incubation, cells were treated with 20 μM GCV for 24 hours and 48 hours. After 24 hours and 48 hours of treatment cells were collected to make lysate. Cell pellets were harvested by centrifugation at 3000 rpm for 5 minutes and washed with ice cold 1X PBS and then re-centrifuged at 3000 rpm for 5minutes. Pellets were resuspended with 200 μl ice cold digitonin permeabilization buffer (1 mM sodium phosphate monobasic, 8 mM sodium phosphate dibasic, 75 mM NaCl, 190 μg/ml digitonin, 250 mM sucrose, protease cocktail inhibitor, pH 7.5) and incubate on ice for 1 hour. After centrifugation at 3000 rpm for 5 minutes at 4 ˚C, 150 μl of supernatant was collected as cytosolic lysate into 1.5 ml pre-chilled microcentrifuge tube. The cells pellets were again washed in ice cold digitonin permeabilization buffer and centrifuged for 3000 rpm for 2 minutes. Washed cells pellets then lysed in 100 μl ice cold RIPA lysis buffer (pierce ™ Ripa buffer, Ref 8990, Thermo Scientific, USA) with 1% phosphatase inhibitor

(04906845001, Roche, Indianapolis, USA) and 1% protease inhibitor cocktail (04693124001, Roche, Manheim, Germany). The resuspended pellets were incubated for 30 minutes on ice and vortexed for 30 seconds every 10 minutes. Then the lysate was centrifuged at 14000 rpm (Centrifuge 5424 R, Eppendorf, Hamburg, Germany) for 10 minutes at 4 °C and collected as mitochondrial lysate into a new pre-chilled 1.5 ml microcentrifuge tubes. For immunoblotting 40 µg of cytosolic lysate and 50 µg of mitochondrial lysate was used. Beta actin and CoxIV were used to confirm equal loading for cytosolic lysate and mitochondrial lysates respectively. For digitonin buffer optimization, GL261 WT, CT2A WT and P3 WT cells were treated with 10 µM Raptinal for 15 minutes and 30 minutes. Untreated WT cells and untreated WT cells with DMSO were used as control.

3.2.3 WST-1 Assay

WST-1 (Cell Proliferation Reagent WST-1, 11644807001, Roche, Mannheim, Germany), is a negatively charged tetrazolium salt. Tetrazolium salt is converted to soluble colored formazan through reduction reaction by mitochondrial dehydrogenase enzymes. This reaction take place only in metabolically active cells, since only live cells carries dehydrogenase enzymes. The amount of formazan production is proportional to the number of metabolically active cells. GL261.TK.GFP, CT2A.TK.GFP and P3.TK.GFP cells were used to perform WST-1 Assay. Cells were seeded in a density of a $1.0x10^4$ /100 µl per well into a 96-well plate (1.5x104 /100 µl for P3 cells) with four replicates. Following overnight incubation, the cells were treated with 20 µM GCV and incubated at 37 °C for 48 hours and 72 hours. After 72 hours incubation, 7 µl of WST-1 was added to each well and incubated at 37 °C. The absorbance was measured after 1.30 hours of incubation with Multiskan™ FC Microplate Photometer (Thermo Fisher Scientific, Massachusetts, USA) at 450 nm. Then the data was analyzed with Excel and plotted in GraphPad prism software.

3.3 Determination of protein concentration

The protein concentration was determined by BCA (bicinchoninic acid) assay using Pierce™ BCA Protein Assay Kit (23225, Thermo scientific, USA). Several concentrations of Bovine serum albumin were used as standard. One part of BCA reagent B was mixed with 50 parts of Reagent A to prepare the working reagent (50:1, Reagent A: B). 200 µl working reagent of Pierce™ BCA reagent is loaded in 96 wells plate/ well and 2 µl of the protein sample was added

to each sample and incubated for 20 minutes at 37 ˚C. Finally, absorbance of protein lysates was measured at 560 nm in a microplate reader Multiskan^{TM} FC Microplate Photometer (Thermo Fisher Scientific, Massachusetts, USA). The data was analyzed, and protein concentration was determined by using a calibration curve.

3.4 Western Immunoblotting

3.4.1 Gel Casting

Polyacrylamide gels were freshly casted. Mostly 10% and 15% gels were used. Resolving gel solution was made by mixing 30% Acrylamide/Bis-acrylamide solution (A3699, Sigma-Aldrich, UK), 1.5 M Tris-HCl (pH 8.8), 10% SDS (w/v), 10% Ammonium Persulfate (APS) (w/v) (A3678, Sigma-Aldrich, St Louis, Missouri, USA), TEMED (T9281, Sigma-Aldrich, UK) and dH2O and the same ingredients were used to prepare 4% stacking gel solution. According to Bio-Rad Hand Casting protocol 1.0M Tris-HCL (pH 6.8) is used instead of 1.5 M Tris-HCL (pH 8.8). For casting gel Mini-PROTEAN® Tetra Hand Cast System (Bio-Rad, Hercules, California, USA) was used.

3.4.2 SDS-PAGE and Sample Preparation

Samples were prepared on ice by mixing protein lysate with LDS Sample Buffer (4x) Bolt TM (Novex, B007, Invitrogen, USA) and NuPage® Sample Reducing Agent (NP0009, Invitrogen, California, USA) and diluted with Milli-Q water to get the desired volume of sample and to ensure the equal protein concentration for every sample. The protein lysate mixtures were then heated for 10 minutes at 70 °C to denature the proteins and spun down for 30 seconds at 14000 rpm. Freshly casted gels were placed in the electrophoresis chamber (Bio-Rad, USA) filled with 1x running buffer (1610732, 10X Tris/Glycine/SDS Buffer, Bio-Rad, USA). The protein lysate mixture was loaded at equal amount into each well and 10 µl of SeeBlue® Plus2 Pre-Stained Protein Standard (LC5925, Invitrogen, California, USA) was used as a molecular marker and loaded into the first well of the gel. After running the gels for approximately 30 minutes at 70V (when all samples were lined up at the stacking-resolving gel separation line), the power was increased to 100V. The gel run was stopped when the protein samples reached the bottom of the gel.

3.4.3 Blotting

After the end of the electrophoretic separation, the separated proteins were transferred onto nitrocellulose membrane (0.2 µm) (10600001, GE Healthcare, Pittsburgh, PA, USA) using electrical current for subsequent analysis. NuPAGE® Technical Guide for electrophoresis system was followed to prepare a blotting sandwich to transfer the protein on the membrane. The blotting sandwich was assembled with a set of blotting sponge pads, filter paper, the SDS-gel, 0.2 µm nitrocellulose membrane in the way shown in Figure 6. Potential air bubbles between the layers were removed by gently rolling with a rolling pin. Immunoblot sandwich was transferred into the XCell II™ Blot Module (EI0001, EI9051, Invitrogen, Carlsbad, California, USA) and inserted into the XCell *SureLock*™ Mini-Cell chamber. The chamber was placed on the ice and fill up with ice cold 1X pre-made transfer buffer. To make 1X transfer buffer, 100 ml of 10X Tris/Glycine Buffer (1610771, BioRad, USA) was added to 700 ml of distilled water and 200 ml of methanol and kept at 4 ˚C. Finally, electrophoresis was run for 90 minutes at 37V by using Invitrogen PowerEase 300W.

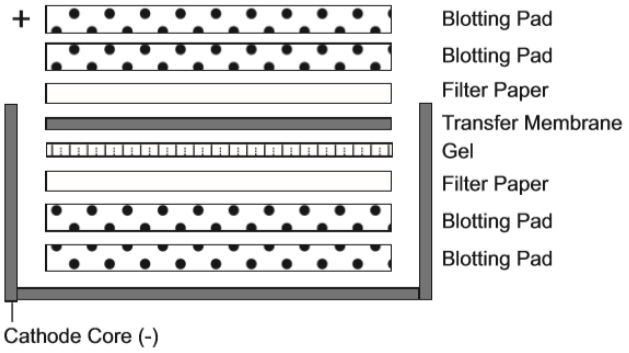

Figure 6 Immunoblot sandwich construction according to the NuPAGE® Technical Guide [65].

3.4.4 Ponceau S staining

After blotting, the nitrocellulose membrane was washed with MilliQ-water and incubated in with 0.1% w/v Ponceau S (P3504, Sigma-Aldrich, St. Louis, Missouri USA) (0.1% w/v Ponceau S in 5% v/v acetic acid) for 5 minutes at room temperature (RT).

3.4.5 Blocking and Antibody Incubation

Wash buffer: 1X TBS-T was used as wash buffer. To prepare 1X TBS, 100 ml of 10X Tris Buffered Saline (TBS) (20 mM Tris-HCl, 0.15 M NaCl, pH 7.6, in distilled water) was diluted with distilled water. After that, 1 ml 0.1% Tween® 20 (9005645, Sigma-Aldrich, St. Louis, Missouri USA) was added. Resulted final buffer 1X TBS with 0.1% Tween 20 was mentioned as TBS-T throughout the thesis.

5% Skim Milk Buffer:

5g of DifcoTM Skim Milk Powder (232100, BD Biosciences, USA) dissolved in 100 ml of TBS-T and used as blocking buffer, as well as antibody diluent.

5% BSA Buffer:

To prepare 5% Bovine Serum Albumin (BSA) buffer, 5 g of BSA (A4503, Sigma-Aldrich, St. Louis, Missouri USA) was dissolve in 100 ml of TBS-T and used as antibody diluent.

After blotting and Ponceau S staining, the membrane was incubated with 5% skim milk TBS-T for 45 minutes at room temperature to block the nonspecific binding site of antibodies on the membrane. Then the membrane was washed 2 times with wash buffer for 3 minutes and incubated with the corresponding primary antibody on a shaker for overnight at 4 ˚C. Primary antibodies were diluted according to the recommended protocol from the manufacturer either in 5% skim milk TBS-T or 5% BSA TBS-T. Next, the membrane was washed 3 times with 1X TBST for 10 minutes each on shaker at room temperature. After that the membrane was incubated with secondary antibody depending on the host species of primary antibody for 1 hour at room temperature (RT). All Secondary antibodies were conjugated with Horseradish Peroxidase (HRP) and were diluted in 5% skim milk TBS-T. After 1 hour incubation, the membrane was washed 5 times with 1X TBS-T for 5 minutes each.

Table 1 Primary and Secondary Antibodies used for Western Immunoblotting

Primary Antibody	Supplier	Catalogue Number	MW (kDa)	Dilution	Host	Buffer
Cytochrome c	Invitrogen USA	MA5-11674	~ 12 kDa	1:500	Mouse	5% skim milk TBS-T
Caspase 9	Cell Signaling USA	9508T	~ 49/39/37(Mouse) kDa ~ 47/37/35(Human) kDa	1:1000	Mouse	5% skim milk TBS-T
Caspase 3	Cell Signaling USA	9664S	~ 19 kDa ~ 17 kDa	1:1000	Rabbit	5% BSA TBS-T
Caspase 8	Novas USA	NB100-56116ss	~ 17-21 kDa ~ 10-13 kDa	1:2000	Rabbit	5% skim milk TBS-T
PARP	Cell Signaling USA	9542S	~ 116 kDa ~ 89 kDa	1:1000	Rabbit	5% BSA TBS-T
COX-IV	Abcam UK	Ab16056	~ 17 kDa	1:2000	Rabbit	5% skim milk TBS-T
Beta actin	Abcam UK	Ab8224	~ 42 kDa	1:2000	Mouse	5% skim milk TBS-T
Secondary Antibody		**Supplier**	**Catalogue Number**	**Dilution**	**Host**	**Buffer**
Goat anti-Mouse IgG (H+L), HRP		Invitrogen USA	31430	1:5000	Mouse	5% skim milk TBS-T
Goat anti-Rabbit IgG (H+L), HRP		Invitrogen USA	31462	1:10000	Rabbit	5% skim milk TBST-T

3.4.6 Protein Detection and Quantification of Protein Expression

The membrane was incubated in the dark with the SuperSignal™ West Pico PLUS Chemiluminescent (34080, Thermo Fisher Scientific, Waltham, USA) for 5 minutes. The Chemiluminescent substrate was prepared by following the manufacturer's recommendation.
A luminescent image analyzer, Image Reader LAS-3000 (Fujifilm Medical System Inc., Connecticut, USA) was used to perform chemiluminescent detection. The images were analyzed with the Image Lab Software (Life Sciences Research, BioRad, USA) and Image J (USA).

3.5 Immunohistochemistry (IHC)

Formalin Fixed Paraffin Embedded (FFPE) brain tumor tissue sections were used in IHC. Before deparaffinization, all the slides were brought from 4 °C to RT and labeled. The slides were deparaffinized by washing 2 times with xylene for 5 minutes, rehydrated with 100%

ethanol and 96% ethanol respectively 2 times for 3 minutes each. Finally, ending in a final rinse with dH20 for 2 minutes.

The slides were then placed at pre-heated (boiling point) citrate buffer (0.01 M citrate buffer with Tween, PH: 6, 7140 Sigma, USA) in a steamer and incubated for 20-25 minutes. After incubation, the container was placed on a bench for 15 minutes to let it cool and washed under running tap water for 10 minutes. Water was wiped off around the tissue sections and the tissue was encircled with ImmEdgeTM Pen (H-4000, VECTOR, USA). Sections were washed 3 times for 5 minutes with TBST-T and blocked for 20 minutes at RT in 5% serum of the host of the secondary antibodies.

After removing the blocking serum and the tissue was incubated with primary antibody in a humidified chamber at 4 °C for overnight. The next day, primary antibody was removed, and the sections were washed 3 times for 5 minutes each with TBS-T and further blocked in 3% hydrogen peroxide (H1009, SIGMA) for 10 minutes at RT. After 10 minutes, again washed 2 times and incubated with biotinylated secondary antibody for 1 hour at RT. ABC complex (VECTASTAINR KIT, 94010, VECTOR, USA) was used to amplify and detect primary. Sections were washed and incubated with ABC complex solution for 30 minutes at RT.

After washing steps of 3 times 5 minutes, visualization was done with 3,3′-diaminobenzidine (DAB) (K3468, DAKO) as substrate under microscope. After staining the target antigen, the sections were stained with hematoxylin for 30 seconds to visualize the nuclei. Hematoxylin was washed thoroughly by H_2O until water is no longer stained blue. Finally, dehydration process was done by washing in dH2O for 2 minutes and incubated in 96% and 100% ethanol for 2 times 3 minutes for each step. The sections were then incubated in xylene for 2 times 5 minutes. Xylene -based permanent mounting medium (HX74982261, Entellan^R New, Germany) was used to mount the sections with cover glass slides. The stained sections were analysed by using a microscope (ECLIPSE E600, Nikon,Japan).

Table 2 Primary and Secondary Antibodies used for Immunohistochemistry (IHC)

Primary Antibody	**Supplier**	**Catalogue Number**	**Dilution**	**Host**	**Buffer**
Caspase 3	Cell Signaling USA	9664S	1:2000	Rabbit	SignalStain® Antibody Diluent (8112, Cell Signaling)
Secondary Antibody	**Supplier**	**Catalogue Number**	**Dilution**	**Host**	**Buffer**
Goat anti-Rabbit IgG (H+L), Biotinylated	Vector Laboratories USA	BA-1000	1:100	Rabbit	0.01 M PBS with 0.05% Tween 20

3.6 luminescence-based caspase-9 and caspase-8 activation assay

The cells were washed, trypsinized and seeded at a density of $1x10^4$ /100 µl per well into a white 96-well plate. After overnight incubation, the cells were treated with 20 µM GCV for 24 hours and 48 hours. Caspase-Glo® 9 Reagent (G8210, Promega, USA) and Caspase-Glo® 8 Reagent (G8201, Promega, USA) were made by following the manufacturer's protocol. 100 µl of Caspase-Glo® 9 Reagent with 60 µM MG-132 was added to each well and gently mixed by using a plate shaker at 300–500 rpm for 30 seconds. To observe the activity of the caspase-8, 100µl of Caspase-Glo® 8 with 60 µM MG-132 was used. MG-132 is a proteasome inhibitor helps to reduce nonspecific background in cell-based assays. Finally, the 96-well plate was covered with aluminum foil to protect from light and incubated at room temperature for 1hour. After 1 hour the luminescence of each sample was measured each sample in a microplate reader TECAN SPARK 20M (Switzerland).

3.7 Statistical Analysis

Prism7.0 GraphPad software was used for statistical analysis. One-way analysis of variance (ANOVA) was used to analyze the results from WST-1 assay and luminescence assay. The mean of each column was compared to the mean of every other column with Tukey. A P-value less than 0.05 have been considered as significant. Quantitative protein expression was normalized to beta actin and fold change was determined to compare untreated with treated sample. Unpaired t-test was used to find the relative band intensity significances for western blot. Asterisk (*) is used for significance and ns is for non-significance.

4.Results

4.1 Glioma cells undergo apoptosis after HSV-TK-mediated suicide gene therapy.

Previously, apoptosis was reported to be a major mode of cell death in several types of cancer cell lines after HSV-TK-mediated suicide gene therapy [66]. However, it is not known if the murine gliomas GL261 and CT2A and most importantly patient-derived stem-like GBM cell lines such as the P3 cell line used in this study, also follow apoptotic pathway in this context. To analyze if these cell lines are sensitive to suicide gene therapy, we treated GL261.TK.GFP, CT2A.TK.GFP and P3.TK.GFP cells with 20 µM concentration of GCV. Untreated TK.GFP cells showed no significant difference in viability, whereas after 48 hours and 72 hours treatment, all the cell lines showed significant cytotoxicity (Figure 7).

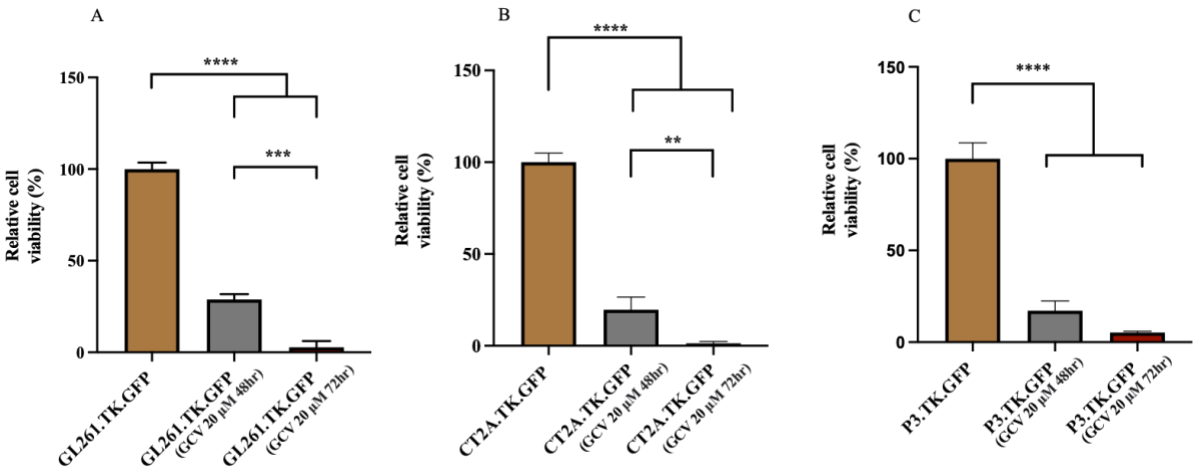

Figure 7 GCV-mediated cytotoxicity in the glioma cells. A. GL261.TK.GFP, B. CT2A.TK.GFP and C. P3.TK.GFP cells are grown as monolayer cultures at 37 °C with 5% CO2 and treated with the GCV at 20 µM concentrations. After 72 hours and 48 hours of incubation, cell viability was investigated by using WST-1 assay. The effect of GCV on cell viability is determined by the comparison of relative cell viability percentage with respect to the untreated TK cells. This represents the result of three independent experiments. For statsticalanalysis one-way Anova with Tukey was used. nsP>0.05, *P<0.05, ** P<0.01, *** P<0.001, **** P<0.0001.

To investigate the mode of cell death in these cells after treating the HSV-TK-transduced tumor cells with GCV, we analysed the cleavage of caspase-3, an enzyme promoting the last step in the apoptotic cascade [49].

Immunoblotting by using an antibody against cleaved caspase-3 revealed that after 24 hours and 48 hours of GCV treatment, the GL261.TK.GFP and CT2A.TK.GFP cells undergo

apoptosis as observed by accumulation of cleaved caspase-3 after 48 hours treatment (Figure 8). Accumulation of cleaved caspase-3 appeared to be low in P3.TK.GFP after 48 hours, however increased 72 hours post-treatment. As positive control, cells were treated with Raptinal. Since Raptinal rapidly triggers apoptosis in cancer cells and demonstrates cleavage of caspase-3 [67]. To quantify the accumulation of cleaved caspase-3, relative band intensity was determined which demonstrated significantly higher accumulation of cleaved caspase-3 in the treated cells (Figure 9).

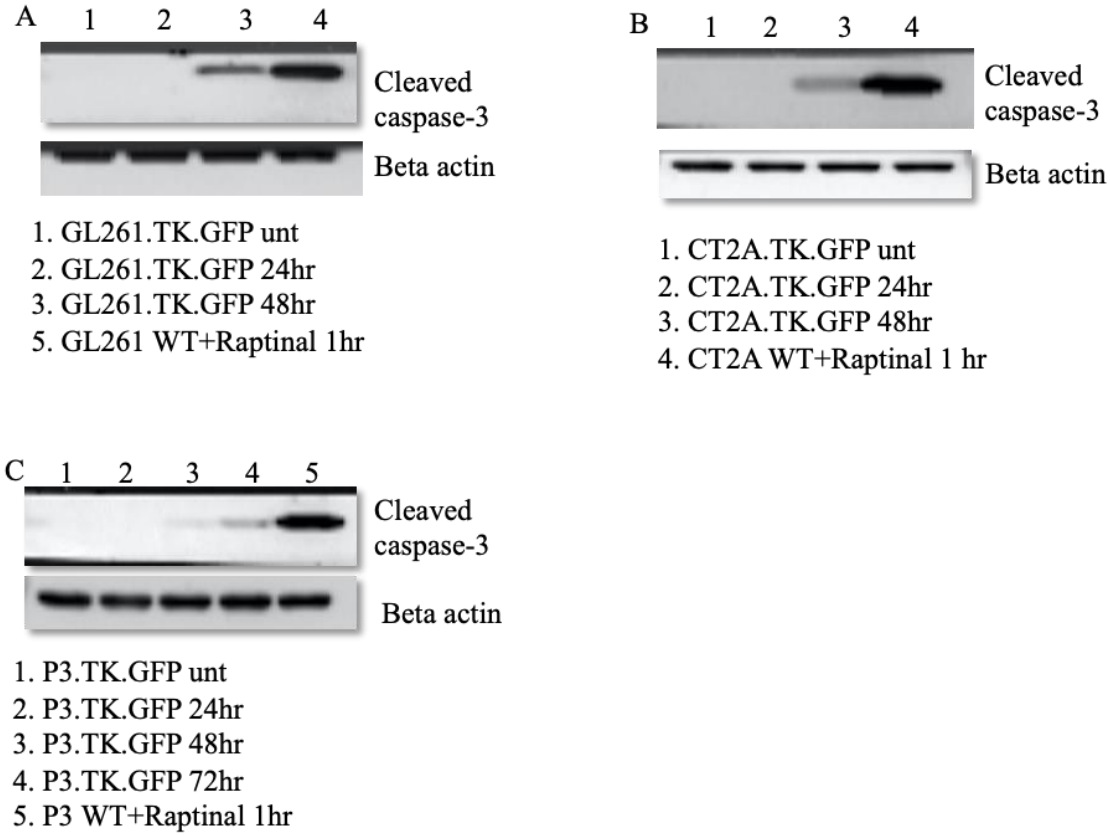

Figure 8 Representative blots show immunoblot analysis of cleaved caspase-3. GL261.TK.GFP, GL261 WT, CT2A.TK.GFP, CT2A WT and P3.TK.GFP, P3 WT cells are grown as monolayer cultures at 37 °C with 5% CO2 and treated with the GCV at 20 μM concentration. Untreated TK.GFP cells were used as control and 10 μM Raptinal treated WT cells were used as positive control. Our result showed the accumulation of cleaved caspase-3 after 48 hours of GCV treatment in A. GL261.TK.GFP and B.CT2A.TK.GFP cell lines. C. In P3.TK.GFP cell line the accumulation of cleaved caspase-3 appeared after 48 hours and 72 hours of treatment. Beta actin was used as loading control. This blot represents three separate experiments.

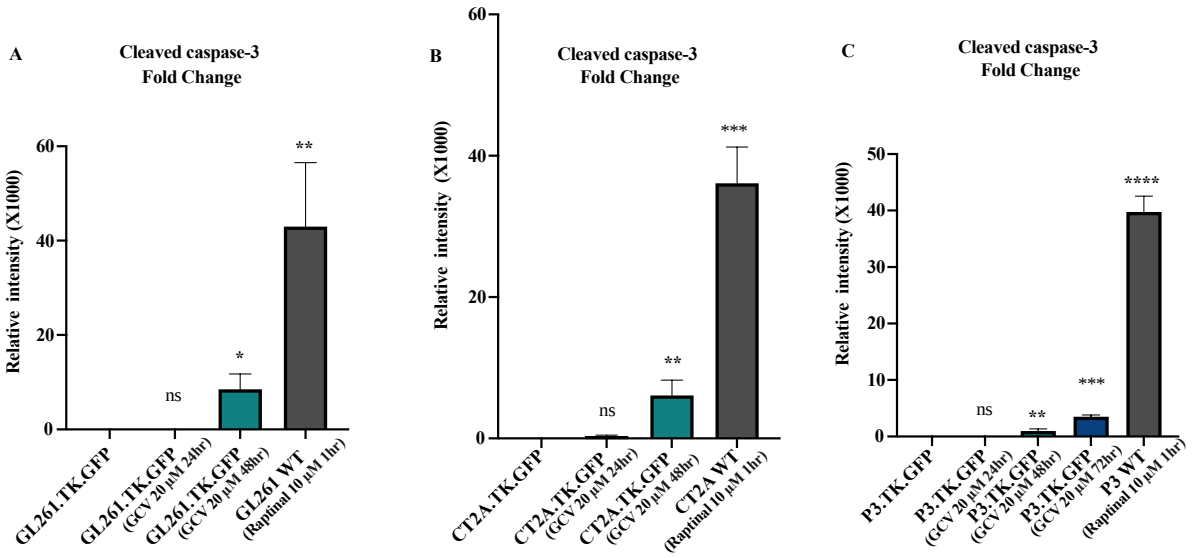

Figure 9 Quantification of cleavage of caspase-3.
Relative band intensity is normalized with beta actin and relative fold change was determined to compare with untreated to the treated sample. In A. GL261.TK.GFP and B. CT2A.TK.GFP the accumulation of cleaved caspase-3 was observed after 48 hours of treatment. The cleavage of caspase-3 was detected in C. P3.TK.GFP after 48 hours and 72 hours of treatment. This result is a representation of three independent experiments. Statistical significance was calculated by using unpaired t-test. $^{ns}P>0.05$, $^{*}P<0.05$, $^{**}P<0.01$, $^{***}P<0.001$, $^{***}P<0.001$.

To further confirm the cleavage of caspase-3, we investigated the presence of cleaved PARP-1. PARP-1 is one of the primary substrates for cleaved caspase-3. We observed that the cleavage of PARP-1 is significantly higher after GCV treatment in all cell lines (Figure 10). Interestingly, also expression of the full-length PARP-1 increased after GCV treatment. In conclusion, we show that the murine glioma cells and P3 undergo apoptosis after GCV treatment.

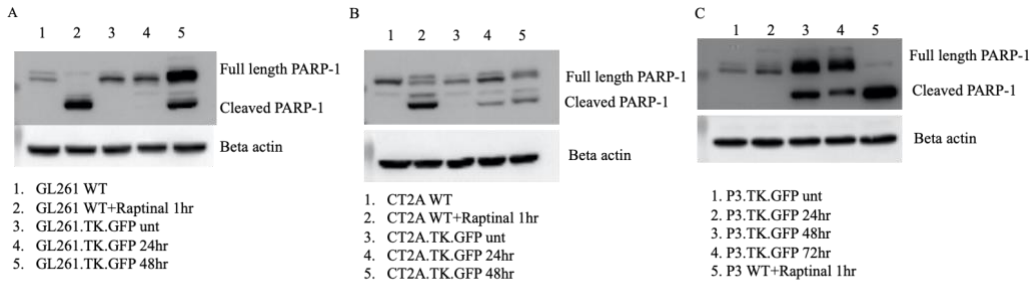

Figure 10 Representative blots show full length PARP-1 and cleaved PARP-1 by immunoblotting assay. GL261.TK.GFP, GL261 WT, CT2A.TK.GFP, CT2A WT and P3.TK.GFP, P3 WT cells are grown as monolayer cultures at 37 °C with 5% CO2. TK expressing cells were treated with the GCV at 20 μM concentration. Untreated cell lysates were used as control. For positive control, 1 hour 10 μM Raptinal treated WT cell lysates were used. A. Significantly increasing amount of cleaved PARP-1 appeared after 48 hours of GCV treatment in

GL261.TK.GFP cells. B. In CT2A.TK.GFP the accumulation of cleaved PARP-1 showed after 24 hours and 48 hours of treatment. C. The cleavage of PARP-1 appeared after 48 hours of treatment but decreased after 72 hours of treatment in P3.TK.GFP cells. Beta actin was used as loading control.

4.2 Apoptosis is detected after HSV-TK mediated gene therapy in vivo

To confirm that apoptosis also occurs in vivo following HSV-TK/GCV treatment we analyzed cleaved caspase-3 in histological brain sections of Gl261 TK- and CT2A TK-bearing mice treated with GCV. Immunohistochemical analyses of the relevant histological sections showed that the untreated tumors, in both models, have very few cells positive for cleaved caspase-3 (Figure 11. A and C). However, in the treatment group, substantial cleavage of caspase-3 is visible (Figure 11. B and D). Thus, we can confirm that the apoptotic pathway observed in the in vitro experiments is also relevant in vivo.

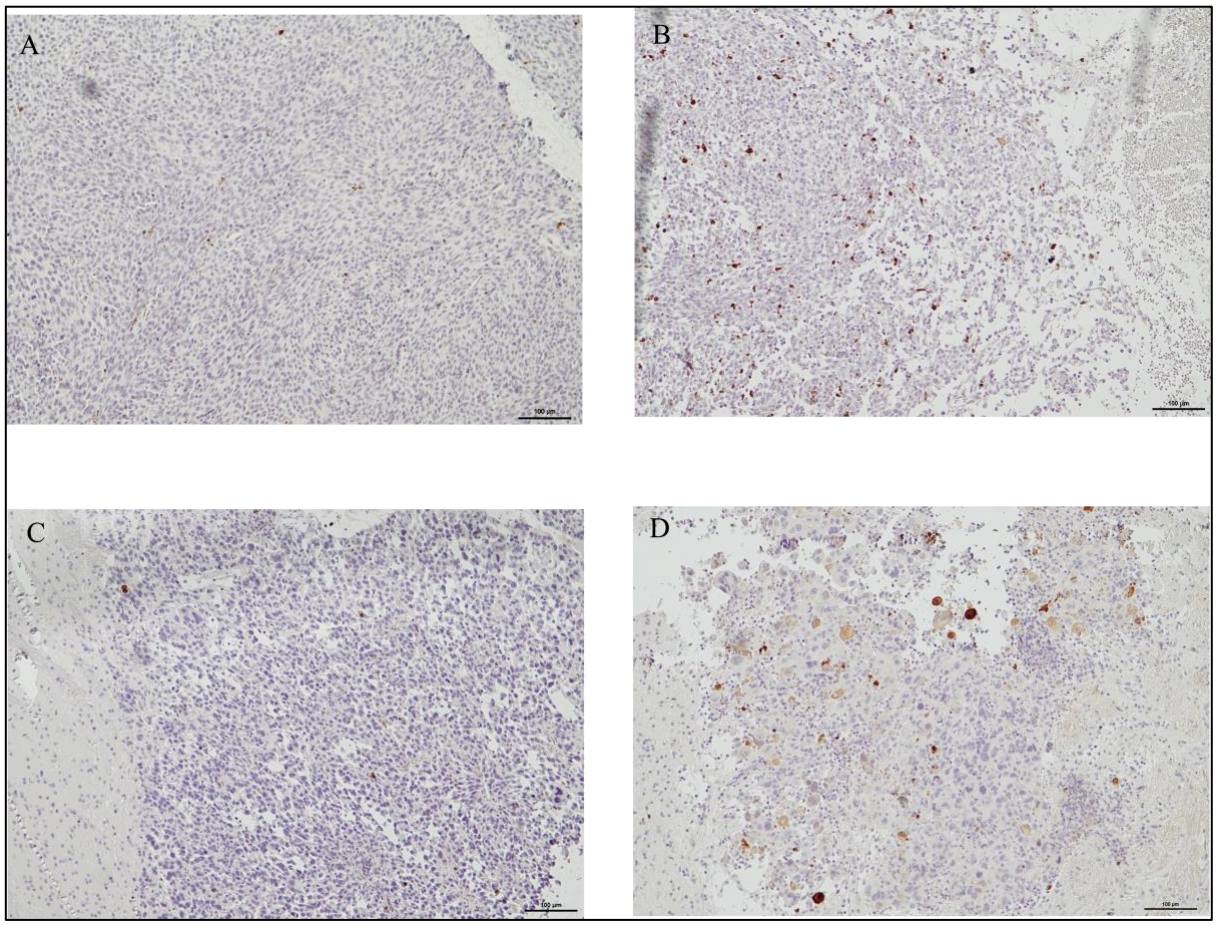

Figure 11 Immunohistochemical staining of cleaved caspase-3 in paraffin-embedded brain sections. Previously, a mixture of WT (70%) and TK.GFP-expressing tumor cells (30%) were implanted orthotopically in syngeneic C57BL/6 mice— CT2A (A, B) and GL261 (C, D). And brains were collected after 5 days (for GL261)

and 3 days (for CT2A) of prodrug treatment. Detection of large amount of apoptotic cells in both CT2A tumor model (B) and GL261 tumor model (D) after treatment compared to the untreated controls respectively (A,C).

4.3 Release of cytochrome c from mitochondria into the cytosol is detected after GCV treatment

To investigate whether intrinsic or extrinsic apoptosis occurs after HSV-TK/GCV, we analyzed the release of cytochrome c from mitochondria into the cytoplasm, which is a key component in the intrinsic apoptotic pathway. Of note, the release of cytochrome c can also be involved in the extrinsic apoptotic pathway through the protein Bid [42].

First, we used a commercial cell fractionation buffer (Cytochrome c Release Apoptosis Assay Kit, QIA87-1KIT, EMD Milipore,USA) to isolate the cytosolic fraction to detect the pool of released cytochrome c. However, we could not detect cytosolic cytochrome c in any of the cell lines (data not shown). Therefore, we adopted and optimized a previously published protocol to prepare digitonin permeabilization buffer in order to extract the cytosolic and mitochondrial lysates [67]. In the wild-type glioma cells which were treated with the positive control Raptinal. Raptinal induces intrinsic apoptosis in which the release of mitochondrial cytochrome c is triggered [67]. We observed that the cytosolic fraction was distinctly enriched with cytochrome c after both 15 minutes and 30 minutes treatment with 10 μM Raptinal in mouse glioma cells (Gl261 WT and CT2A WT) and after 30 minutes in human glioma cells (P3 WT; Figure 12).

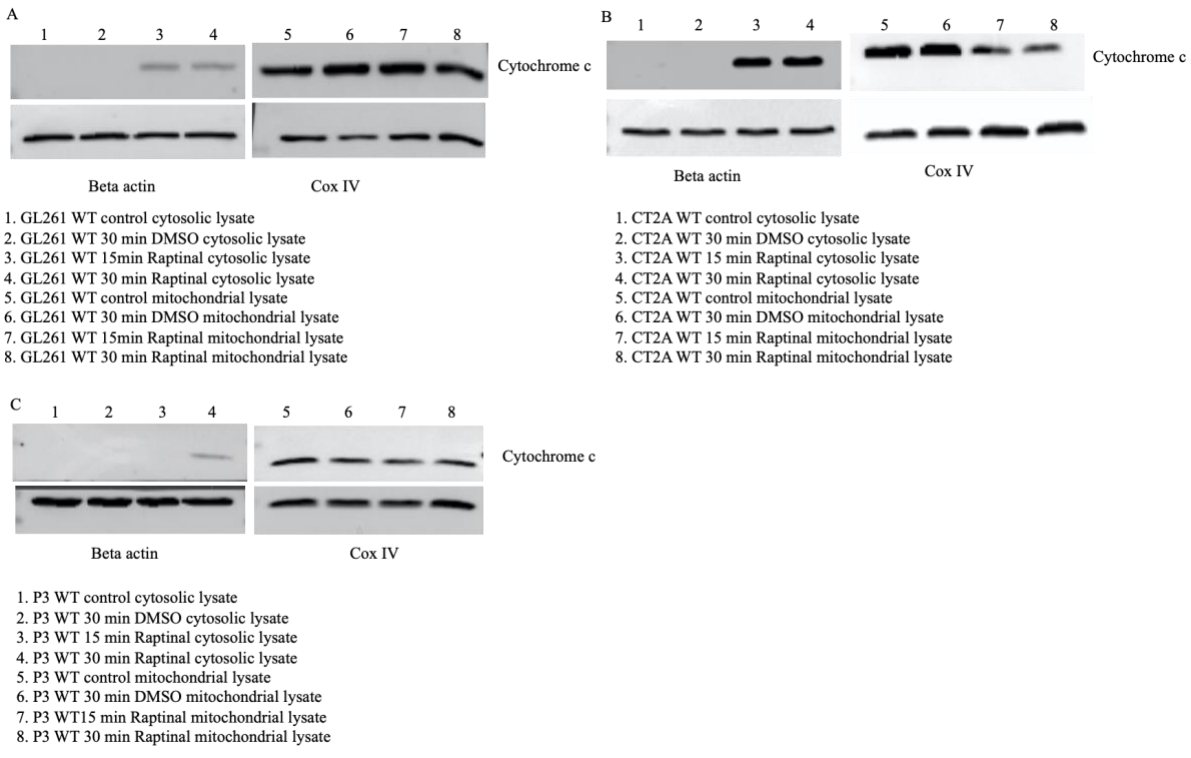

Figure 12: Representative blots show cytosolic and mitochondrial cytochrome c in WT cells after Raptinal treatment. Gl261 WT, CT2A WT and P3 WT cells were grown and maintained in 37 °C with 5% CO2. These cells were treated with 10 µM Raptinal for 15 minutes and 30 minutes. Digitonin permeabilization buffer was used to extract cytosolic fraction after treatment. Untreated cells and cells treated with DMSO were used as control and compared with treated cells. A. In GL261 WT, B. CT2A WT glioma cells cytochrome c was detected after 15 minutes and 30 minutes treatment, C. But in P3 WT cells cytochrome c was found after 30 minutes treatment. Beta- actin was used as loading control for cytosolic fraction and Cox IV was used for mitochondrial loading control.

After confirmation that the buffer was working, we analyzed the presence of cytochrome c in GL261.TK.GFP, CT2A.TK.GFP, P3.TK.GFP cells following GCV treatment. Cytochrome c was detected in all cell lines in the mitochondrial fraction. However, only the mouse glioma cell lines GL261.TK.GFP, CT2A.TK.GFP, showed a significant accumulation of cytosolic cytochrome c in the cytosolic fraction after 24 hours treatment (Figure 13). The release of cytochrome c in the cytosolic fraction was not detected in P3.TK.GFP.

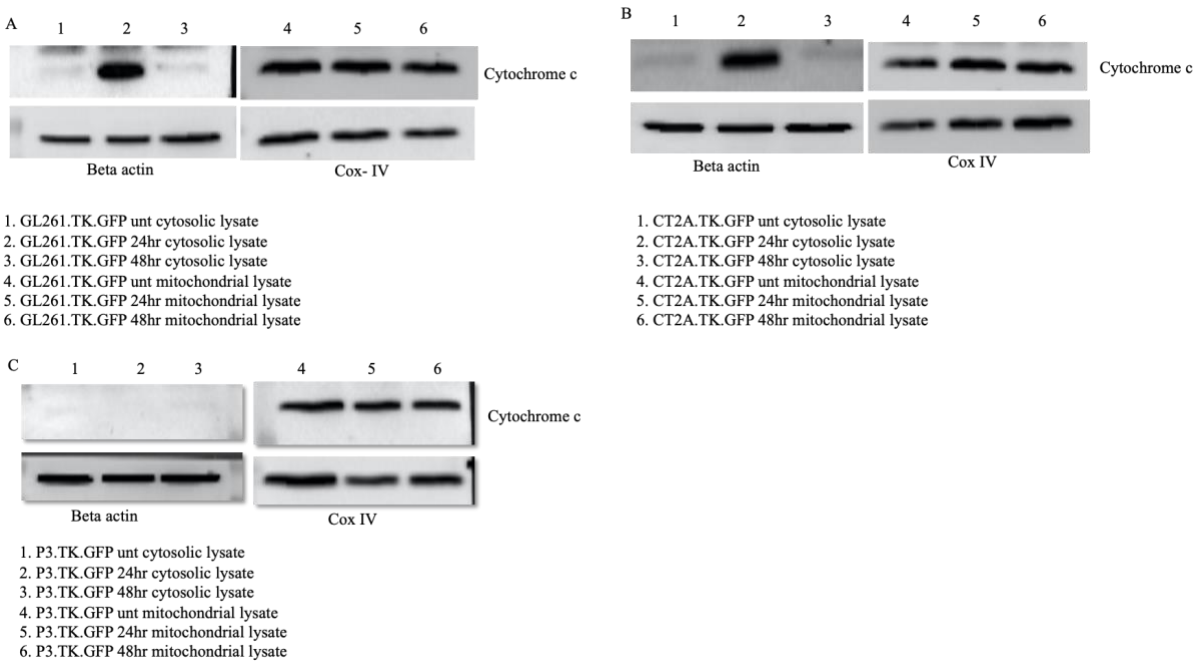

Figure 13 Representative blots show cytosolic and mitochondrial cytochrome c after treatment of GCV. The GL261.TK.GFP, CT2A.TK.GFP and P3.TK. GFP cells were treated with 20 µM GCV for 24 hours and 48 hours. A. significantly increasing amount of cytosolic cytochrome c was observed in GL261.TK.GFP after 24 hours of GCV treatment. B. In CT2A.TK.GFP the cytosolic cytochrome c was also appeared after 24 hours of GCV treatment. C. However, the cytosolic cytochrome c was not appeared after treatment condition in P3.TK.GFP cells. The amount of cytochrome c in the mitochondrial fraction was unchanged in all the cell lines that was used. Beta actin and Cox IV was used as cytosolic loading control and mitochondrial loading control.

4.4 Intrinsic apoptotic pathway is activated after HSV-TK/GCV treatment

The release of cytochrome c from mitochondria to cytosol initiates activation of initiator caspases in mammalian cells. To investigate if the intrinsic pathway is successfully activated after cytochrome release, we analyzed the activation of initiator caspase-9 in the same three cell lines. A significantly higher amount of cleaved caspase-9 was observed after 48 hours of GCV treatment in the GL261.TK.GFP and CT2A.TK.GFP cell lines (Figure 14). Also P3.TK.GFP cells showed accumulation of cleaved caspase-9, however after 72 hours of GCV treatment. As positive control, cells were treated with Raptinal. Since Raptinal rapidly triggers intrinsic apoptosis in cancer cells [67]. To quantify the accumulation of cleaved caspase-9, relative band intensity was determined which demonstrated significantly higher accumulation of cleaved caspase-9 in the treated cells (Figure 15).

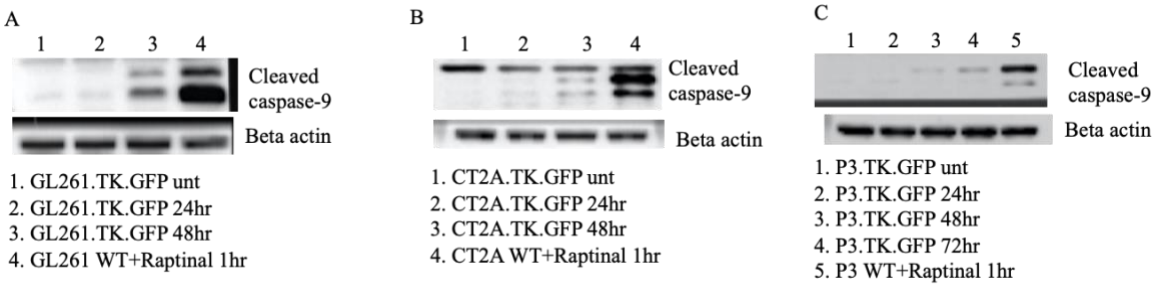

Figure 14 Representative blots show accumulation of cleaved caspase-9 by immunoblotting.
GL261.TK.GFP, Gl261 WT, CT2A.TK.GFP, CT2A WT and P3.TK.GFP, P3 WT cells are grown as monolayer cultures at 37 °C with 5% CO2. TK expressing cells were treated with 20 μM GCV and WT cells were treated with 10 μM Raptinal. Raptinal treated cell lysates were used as a positive control and untreated TK expressing cells used as a control. The accumulation of cleaved caspase-9 was observed after 48 hours of GCV treatment in A. GL262.TK.GFP and B. CT2A.TK.GFP cell lines. C. In P3.TK.GFP the cleavage of caspase-9 appeared after 48 hours but the accumulation of cleaved caspase-9 was very low. After 72 hours of GCV treatment significantly increasing amount of cleaved caspase-9 was detected. Beta actin was use as a loading control.

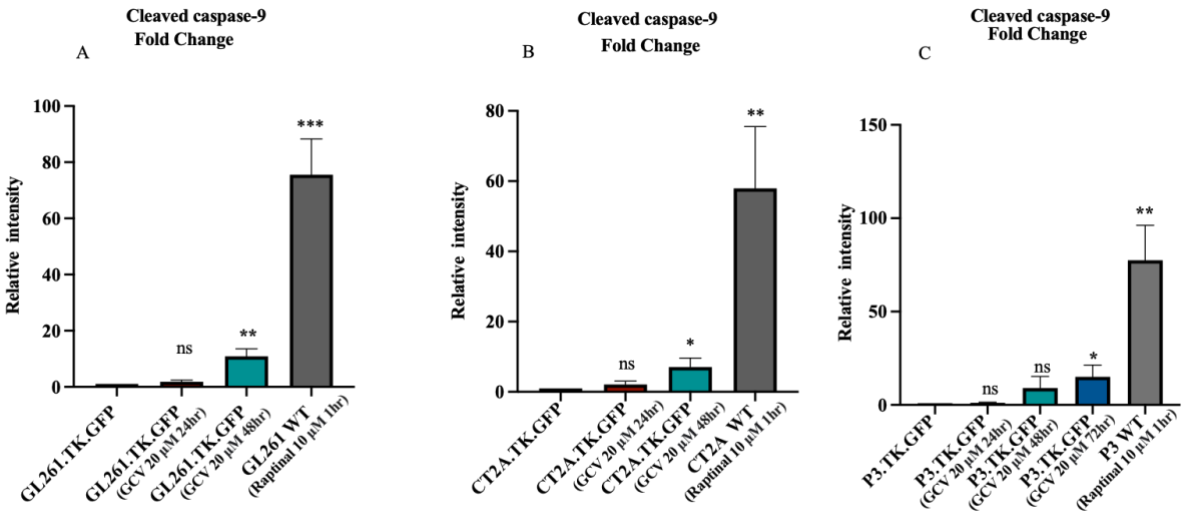

Figure 15 Quantification of cleaved caspase-9. Quantitative cleavage of caspase-9 was normalized with beta actin to calculate the fold change. This result is a representation of three independent experiments. A. in Gl261.TK.GFP significantly increase amount of cleaved caspase-9 was observed after 48 hours of GCV treatment. B. The same pattern was also observed in B. CT2A.TK.GFP. C. In P3.TK.GFP higher accumulation of cleaved caspase was detected after 72 hours of treatment. Fold change was determined by the comparison of relative cleavage of caspase-9 with the respect to the untreated TK cells. Unpaired t-test was used to analyze statistical significance ns P>0.05, *P<0.05, ** P<0.01, *** P<0.001.

We have employed a direct caspase-9 activation luminescence assay in the same cell lines and condition to validate the outcome from the immunoblotting. During the assay we have used a proluminogenic caspase-9 substrate aminoluciferin containing LEHD sequence which is cleaved by caspase-9 resulting release of aminoluciferin which upon action of luciferase produces a “glow-type” luminescent signal. The detected signal is proportional to the amount of caspase activity present. The activation of caspase-9 was detectable after 24 hours of GCV treatment in GL261.TK.GFP cells and decreased after 48 hours. In CT2A.TK.GFP, the activity of caspase-9 was higher at 48 hours compared to 24 hours. In P3.TK.GFP cells, caspase-9 activity was also detected after 24 hours of GCV treatment and gradually increase after 48 hours and 72 hours of treatment. Thus, we can confirm that intrinsic apoptosis was activated in all cell lines (Figure 16).

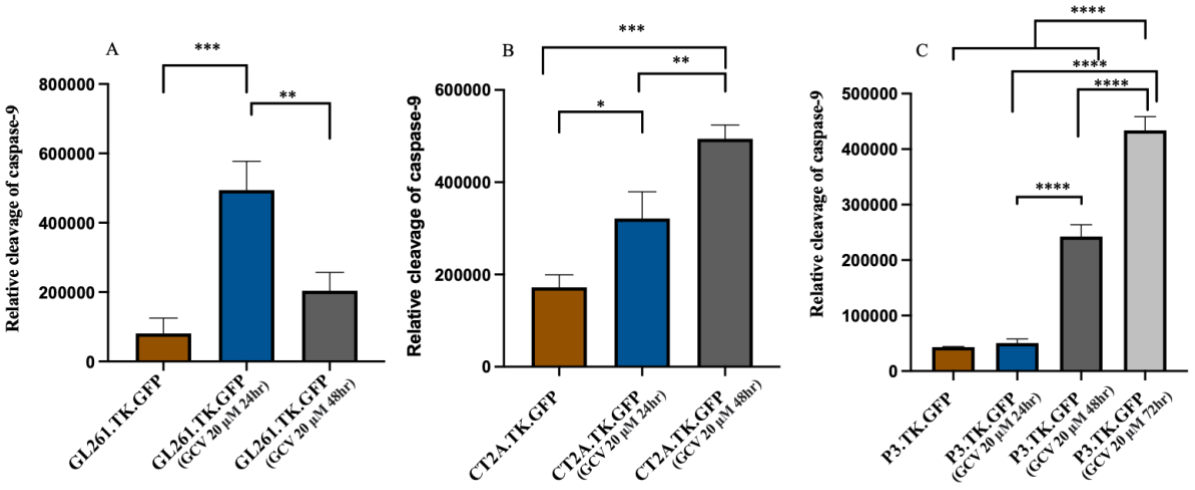

Figure 16 Representative blots showed direct caspase-9 activation assay. GL261.TK.GFP, CT2A.TK.GFP and P3.TK.GFP cells are grown as monolayer cultures at 37 °C with 5% CO2 and treated with the GCV at 20 μM concentrations. A. In GL261.TK.GFP cells the activation of cleaved caspase-9 was found after 24 hours treatment but decreased after 48 hours of post treatment. B. In CT2A.TK.GFP gradually increasing pattern of cleaved caspase was detected after 24 hours and 48 hours treatment. C. In P3.TK.GFP cells, an increased level of cleaved caspase-9 was also observed after 48 hours and 72 hours of treatment. The relative cleavage of caspase-9 was determined by the comparison of untreated to treated cells. The result represents three independent experiments with three replicates. For statistical analysis one-way Anova with Tukey was used. nsP>0.05, *P<0.05, ** P<0.01, *** P<0.001, **** P<0.0001.

4.5 Extrinsic apoptosis is also activated after HSV-TK/GCV treatment

In principle, cells can simultaneously undergo both intrinsic and extrinsic apoptosis. Therefore, it is also important to analyze the involvement of extrinsic apoptosis in the glioma cell lines during suicide gene therapy. As cleaved caspase-8 is the initiator caspase for extrinsic apoptosis, we analyzed the proteolytic cleavage of caspase-8 by immunoblotting using antibodies against cleaved caspase-8. After GCV treatment the accumulation of cleaved caspase-8 was not observed in any of the cell lines. However, we also failed to detect the full-length caspase-8 (Figure 17).

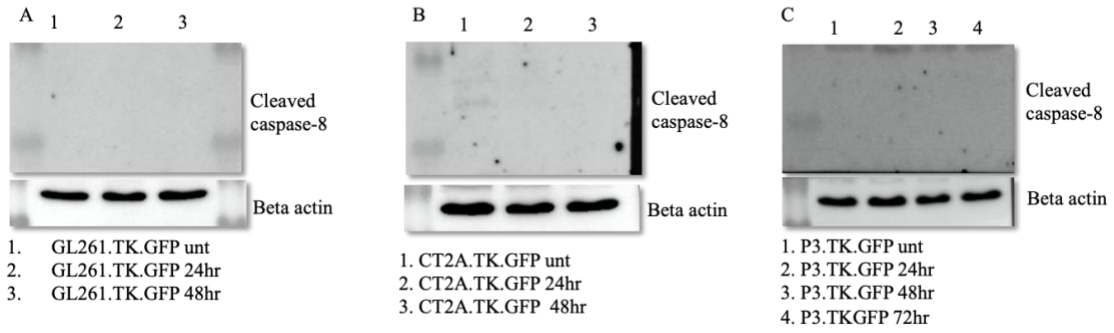

Figure 17 Representative blots show the cleavage of caspase-8. GL261.TK.GFP, CT2A.TK.GFP and P3.TK.GFP cells were grown as monolayer cultures at 37 °C with 5% CO2 and treated with the 20 μM GCV. The cleavage of caspase-8 was analyzed by immunoblotting. The accumulation of cleaved caspase-8 was not detected in A. GL261.TK.GFP, B. CT2A.TK.GFP and C. P3.TK.GFP cell lines. Beta actin was used as loading control.

Due to the difficulty in finding an efficient antibody for immunoblotting cleaved caspase-8 and cleavage therefore, we used a luminescence activation assay similar to the one for caspase 9 activation. To determine caspase-8 activity a proluminogenic caspase-8 substrate aminoluciferin with LETD sequence instead of caspase-9 aminoluciferin substrate with LEHD sequence was used. The activation of caspase-8 was gradually increased after 24 hours and 48 hours of GCV treatment in B. CT2A.TK.GFP. C. In P3.TK.GFP cell lines the activation of cleaved caspase-8 was observed after 24 hours of treatment and followed the increasing pattern after 48 hours and 72 hours of treatment (Figure 18). A significantly higher amount of cleaved caspase-8 was detected in A. GL261.TK.GFP cells after 24 hours but decreased after 48 hours of GCV treatment. This result suggest that the activation of extrinsic cell death also occurs in parallel to the intrinsic pathway.

.

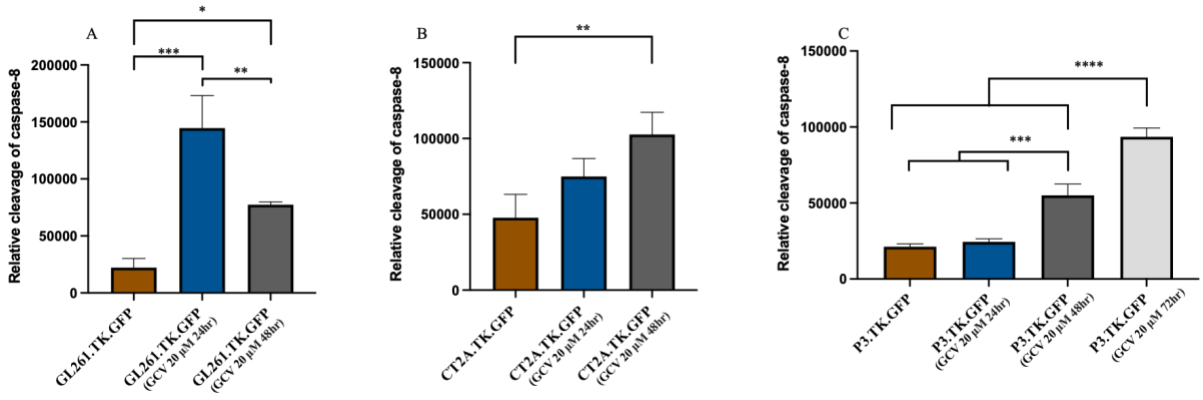

Figure 18 Representative blots show direct caspase-8 activation assay. GL261.TK.GFP, CT2A.TK.GFP and P3.TK.GFP cells were grown as monolayer cultures at 37 °C with 5% CO2 and treated with the GCV at 20 μM concentrations. A. in GL261.TK.GFP cells the activation of cleaved caspase-8 was significantly high after 24 hours treatment. B. In CT2A.TK.GFP gradually increasing amount of cleaved caspase-8 was observed after 24 hours and 48 hours of GCV treatment. C. In P3.TK.GFP cells an increased level of cleaved caspase-8 was observed after 48 hours and 72 hours of treatment. The relative accumulation of cleaved caspase-8 was determined by the comparison of respect to untreated cells. The result represents three independent experiments with three replicates. For statistical analysis one-way Anova with Tukey was used. nsP>0.05, *P<0.05, ** P<0.01, *** P<0.001, **** P<0.0001

5. Discussion

Suicide gene therapy by using HSV-TK/GCV treatment is one of the most popular gene therapy systems used experimentally for the treatment of GBM [68]. Despite very promising results in preclinical models and also in some small scale clinical trials, this therapy has mostly failed to show significantly increased survival in large-scale clinical trials [68]. Lack of reliable preclinical model systems, inefficiency of some of the viral vectors and lack of immunogenic nature have been thought to be the reason behind the failure [68].

In this context, multiple studies are currently being undertaken in our laboratory to understand the immunogenic nature of the cell death triggered by the HSV-TK/GCV system. Theoretically, the mode of cell death can impact the tumor immune microenvironment and thereby also influence the therapeutic outcome. Independent of the immune system, the mechanism of cell death can also influence the efficacy of the therapy. Therefore, it is crucial to know the cell death mechanism following HSV-TK/GCV treatment.

Research over the last decades suggests that HSV-TK/GCV can trigger distinctive [66] cell death pathways including apoptosis in cancer cells [69]. Although some glioma cells are known to activate apoptosis after HSV-TK/GCV treatment, detailed and deeper understandings of cell death mechanism is still missing. In particular, patient derived stem-like GBM cell lines have not been investigated in this context. These cell lines represent geno-and phenotype of the patients and are thus currently the best models available for GBM research [70].

Previous experiments performed in our laboratory by using in vivo syngeneic models with CT2A and GL261 showed that HSV-TK/GCV therapy can result in significant survival benefit in the GL261 model but cannot cure the animals and fails to demonstrate long term survival. Interestingly the same therapy is very efficient in the CT2A model and can completely cure the tumor-bearing mice (unpublished observation). This contrasting result can potentially be associated with distinctive mechanisms of cell death following HSV-TK/GCV treatment. It is well-known that apoptotic cell death is anti-inflammatory and tolerogenic, while some other types of cell death mechanisms, such as necroptosis and pyroptosis promote inflammation. Thus, the interesting result in terms of contrasting survival has prompted us to investigate the cell death mechanism in these two cells lines with HSV-TK/GCV mediated suicide gene therapy treatment. The inclusion of the P3 cell line is justified by the fact that almost nothing is known about the cell death mechanism in patient derived stem like GBM cells. In addition, P3

has been previously vigorously tested in pre-clinical animal studies which show that HSV-TK/GCV therapy is highly effective in this model [61].

Our experimental data show that apoptotic cell death is activated in all these cell lines after HSV-TK/GCV treatment by activation of caspase-3/cleavage of PARP-1. Initiation of apoptosis in this treatment setting was also confirmed in histological brain sections of syngeneic murine glioma models GL261 and CT2A.

The apoptotic cell death process can be initiated either with the extrinsic (death receptor pathway) or the intrinsic (mitochondrial pathway) routes. Our data confirms the presence of cytosolic cytochrome c and subsequently accumulation of cleaved caspase-9 after GCV treatment in GL261.TK.GFP and CT2A.TK.GFP cells [71]. Furthermore, we were also able to demonstrate the activation of caspase-8 in these cell lines, which indicates parallel involvement of the extrinsic apoptotic pathway. Similar phenomenon is also observed in Chemotherapy-induced apoptosis in hepatocellular carcinoma [72]. Cross talk between extrinsic and intrinsic apoptotic pathway is known to exist. Bid, a Bcl-2 family protein, plays main role in this scenario. The activated caspase-8 intersects the intrinsic pathway by cleaving the pro-apoptotic protein Bid resulting in tBid. tBid triggers mitochondrial MOMP and subsequent activation of the caspase cascade [73]. Thus, in future, it would be interesting to investigate whether and when bid is activated during suicide gene therapy.
Interestingly, cytochrome c was not detected in the human glioma P3.TK.GFP cells although cleavage of caspase-9 was observed. It is not clear if and how the intrinsic pathway is activated in this cell line without the involvement of cytochrome c release. So further investigation is necessary to reveal the cell death mechanisms in patient derived human glioblastoma cells. This can be achieved by using specific inhibitors which are directed against caspase-9, caspase-8 or caspase-3 [74]. Such an experiment will be important.

Another important observation is that the activation of caspase-9 and caspase-8 was detected earlier in the direct activation assays compared to the immunoblotting assay. It will be important to investigate this discrepancy further in details.

In this thesis one of the major limitations is that we could not detect cleaved caspase-8 in our samples by immunoblotting analysis. In future it would be essential to confirm the activation of caspase-8 by another assay to strengthen the observation of luminescence-based caspase-8 activation assay. Due to the shortage of time, we have also failed to study the involvement of

caspase-2. Caspase-2 is the most evolutionarily conserved mammalian caspase and demonstrates both positive and negative regulatory functions in apoptosis depending on the cell type, state of growth, and death stimuli. It has been shown that caspase-2 can act upstream of both intrinsic and extrinsic apoptotic pathways [75]. In future one should investigate the activation of caspase-2 and its role in HSV-TK-mediated suicide gene therapy treatment in glioblastoma cells to reveal the complete mechanism of cell death.

Another interesting finding in this work is the overexpression of full-length PARP-1after HSV-TK/GCV treatment in P3.TK.GFP and GL261.TK.GFP cells. This upregulation of PARP-1 may represent a compensatory mechanism for the increasing levels of DNA damage [76]. If so, combination of PARP-inhibition may be useful for HSV-TK gene therapy. PARP inhibition has been considered as a novel approach to suppress DNA repair and promote apoptosis in cells that are treated with specific anticancer agents [77]. It also increases the cytotoxicity of DNA-damaging agents such as temozolomide [78].Thus, in the future, the role of PARP inhibitors in suicide gene therapy of gliomas should be investigated.

Overall, our experimental data confirm apoptosis activation in our cell lines. However, in cancer therapy multiple mechanisms of cell death can also be involved simultaneously [79] [80].Thus, it is important to investigate if HSV-TK/GCV mediated gene therapy, apart from apoptosis, can trigger other cell death mechanisms such as autophagy, necroptosis, ferroptosis and pyroptosis.

6. Conclusion

In this study we have shown that HSV-TK/GCV mediated suicide gene therapy induces apoptosis in mouse glioma cell lines as well as in the patient derived P3 glioblastoma cell line. Our results also indicate that both, intrinsic and extrinsic apoptotic pathways are activated in these cell lines under suicide gene therapy. However, this needs to be confirmed with additional experiments in the future.

7. Reference

1. Pecorino, L., *Molecular biology of cancer : mechanisms, targets, and therapeutics*. 2021.
2. Hanahan, D. and R.A. Weinberg, *The hallmarks of cancer.* Cell, 2000. **100**(1): p. 57-70.
3. Hanahan, D. and R.A. Weinberg, *Hallmarks of cancer: the next generation.* Cell, 2011. **144**(5): p. 646-74.
4. (MFMER), M.F.f.M.E.a.R., *Brain metastases.* Dec. 12, 2020.
5. Walker, D., et al., *Strategies to accelerate diagnosis of primary brain tumors at the primary-secondary care interface in children and adults.* CNS Oncol, 2013. **2**(5): p. 447-62.
6. Ostrom, Q.T., et al., *CBTRUS Statistical Report: Primary Brain and Central Nervous System Tumors Diagnosed in the United States in 2008-2012.* Neuro Oncol, 2015. **17 Suppl 4**: p. iv1-iv62.
7. Adamson, C., et al., *Glioblastoma multiforme: a review of where we have been and where we are going.* Expert Opin Investig Drugs, 2009. **18**(8): p. 1061-83.
8. Wen, P.Y. and S. Kesari, *Malignant gliomas in adults.* N Engl J Med, 2008. **359**(5): p. 492-507.
9. Thakkar, J.P., et al., *Epidemiologic and molecular prognostic review of glioblastoma.* Cancer Epidemiol Biomarkers Prev, 2014. **23**(10): p. 1985-96.
10. Kwiatkowska, A., et al., *Strategies in gene therapy for glioblastoma.* Cancers (Basel), 2013. **5**(4): p. 1271-305.
11. Ohgaki, H. and P. Kleihues, *Epidemiology and etiology of gliomas.* Acta Neuropathol, 2005. **109**(1): p. 93-108.
12. Urbanska, K., et al., *Glioblastoma multiforme - an overview.* Contemp Oncol (Pozn), 2014. **18**(5): p. 307-12.
13. Ohgaki, H. and P. Kleihues, *The definition of primary and secondary glioblastoma.* Clin Cancer Res, 2013. **19**(4): p. 764-72.
14. Cancer Genome Atlas Research, N., *Comprehensive genomic characterization defines human glioblastoma genes and core pathways.* Nature, 2008. **455**(7216): p. 1061-8.
15. Alifieris, C. and D.T. Trafalis, *Glioblastoma multiforme: Pathogenesis and treatment.* Pharmacol Ther, 2015. **152**: p. 63-82.

16. Carlsson, S.K., S.P. Brothers, and C. Wahlestedt, *Emerging treatment strategies for glioblastoma multiforme.* EMBO Mol Med, 2014. **6**(11): p. 1359-70.
17. Wang, J.S., H.J. Wang, and H.L. Qian, *Biological effects of radiation on cancer cells.* Mil Med Res, 2018. **5**(1): p. 20.
18. Baskar, R., et al., *Biological response of cancer cells to radiation treatment.* Front Mol Biosci, 2014. **1**: p. 24.
19. Davis, M.E., *Glioblastoma: Overview of Disease and Treatment.* Clin J Oncol Nurs, 2016. **20**(5 Suppl): p. S2-8.
20. Zhang, J., M.F. Stevens, and T.D. Bradshaw, *Temozolomide: mechanisms of action, repair and resistance.* Curr Mol Pharmacol, 2012. **5**(1): p. 102-14.
21. Pegg, A.E., *Mammalian O6-alkylguanine-DNA alkyltransferase: regulation and importance in response to alkylating carcinogenic and therapeutic agents.* Cancer Res, 1990. **50**(19): p. 6119-29.
22. Baer, J.C., et al., *Depletion of O6-alkylguanine-DNA alkyltransferase correlates with potentiation of temozolomide and CCNU toxicity in human tumour cells.* Br J Cancer, 1993. **67**(6): p. 1299-302.
23. Cai, X. and M.E. Sughrue, *Glioblastoma: new therapeutic strategies to address cellular and genomic complexity.* Oncotarget, 2018. **9**(10): p. 9540-9554.
24. Meacham, C.E. and S.J. Morrison, *Tumour heterogeneity and cancer cell plasticity.* Nature, 2013. **501**(7467): p. 328-37.
25. Robbins, P.D. and S.C. Ghivizzani, *Viral vectors for gene therapy.* Pharmacol Ther, 1998. **80**(1): p. 35-47.
26. Okura, H., C.A. Smith, and J.T. Rutka, *Gene therapy for malignant glioma.* Mol Cell Ther, 2014. **2**: p. 21.
27. Tobias, A., et al., *The art of gene therapy for glioma: a review of the challenging road to the bedside.* J Neurol Neurosurg Psychiatry, 2013. **84**(2): p. 213-22.
28. Duarte, S., et al., *Suicide gene therapy in cancer: where do we stand now?* Cancer Lett, 2012. **324**(2): p. 160-70.
29. Hossain, J.A., et al., *Lentiviral HSV-Tk.007-mediated suicide gene therapy is not toxic for normal brain cells.* J Gene Med, 2016. **18**(9): p. 234-43.
30. Preuss, E., et al., *Cancer suicide gene therapy with TK.007: superior killing efficiency and bystander effect.* J Mol Med (Berl), 2011. **89**(11): p. 1113-24.
31. Karjoo, Z., X. Chen, and A. Hatefi, *Progress and problems with the use of suicide genes for targeted cancer therapy.* Adv Drug Deliv Rev, 2016. **99**(Pt A): p. 113-128.

32. Alberts, B., *Molecular biology of the cell, 5th edition*. 2008, New York: Garland Science.
33. Mesnil, M., et al., *Bystander killing of cancer cells by herpes simplex virus thymidine kinase gene is mediated by connexins.* Proc Natl Acad Sci U S A, 1996. **93**(5): p. 1831-5.
34. McCormick, F., *Cancer gene therapy: fringe or cutting edge?* Nat Rev Cancer, 2001. **1**(2): p. 130-41.
35. Ellis, H.M. and H.R. Horvitz, *Genetic control of programmed cell death in the nematode C. elegans.* Cell, 1986. **44**(6): p. 817-29.
36. Elmore, S., *Apoptosis: a review of programmed cell death.* Toxicol Pathol, 2007. **35**(4): p. 495-516.
37. Kaur, J. and J. Debnath, *Autophagy at the crossroads of catabolism and anabolism.* Nat Rev Mol Cell Biol, 2015. **16**(8): p. 461-72.
38. Galluzzi, L., et al., *Molecular mechanisms of cell death: recommendations of the Nomenclature Committee on Cell Death 2018.* Cell Death Differ, 2018. **25**(3): p. 486-541.
39. Tang, D., et al., *The molecular machinery of regulated cell death.* Cell Res, 2019. **29**(5): p. 347-364.
40. Galluzzi, L., et al., *Essential versus accessory aspects of cell death: recommendations of the NCCD 2015.* Cell Death Differ, 2015. **22**(1): p. 58-73.
41. Schattenberg, J.M., P.R. Galle, and M. Schuchmann, *Apoptosis in liver disease.* Liver Int, 2006. **26**(8): p. 904-11.
42. Pistritto, G., et al., *Apoptosis as anticancer mechanism: function and dysfunction of its modulators and targeted therapeutic strategies.* Aging (Albany NY), 2016. **8**(4): p. 603-19.
43. Aizawa, S., G. Brar, and H. Tsukamoto, *Cell Death and Liver Disease.* Gut Liver, 2020. **14**(1): p. 20-29.
44. Shi, Y., *Mechanisms of caspase activation and inhibition during apoptosis.* Mol Cell, 2002. **9**(3): p. 459-70.
45. Julien, O. and J.A. Wells, *Caspases and their substrates.* Cell Death Differ, 2017. **24**(8): p. 1380-1389.
46. Li, J. and J. Yuan, *Caspases in apoptosis and beyond.* Oncogene, 2008. **27**(48): p. 6194-206.

47. Van Opdenbosch, N. and M. Lamkanfi, *Caspases in Cell Death, Inflammation, and Disease.* Immunity, 2019. **50**(6): p. 1352-1364.
48. Yu, P., et al., *Pyroptosis: mechanisms and diseases.* Signal Transduct Target Ther, 2021. **6**(1): p. 128.
49. Fan, T.J., et al., *Caspase family proteases and apoptosis.* Acta Biochim Biophys Sin (Shanghai), 2005. **37**(11): p. 719-27.
50. Green, D.R. and G. Kroemer, *The pathophysiology of mitochondrial cell death.* Science, 2004. **305**(5684): p. 626-9.
51. Danial, N.N. and S.J. Korsmeyer, *Cell death: critical control points.* Cell, 2004. **116**(2): p. 205-19.
52. Slee, E.A., C. Adrain, and S.J. Martin, *Serial killers: ordering caspase activation events in apoptosis.* Cell Death Differ, 1999. **6**(11): p. 1067-74.
53. Kuribayashi, K., P.A. Mayes, and W.S. El-Deiry, *What are caspases 3 and 7 doing upstream of the mitochondria?* Cancer Biol Ther, 2006. **5**(7): p. 763-5.
54. Green, D.R., *The Coming Decade of Cell Death Research: Five Riddles.* Cell, 2019. **177**(5): p. 1094-1107.
55. Danial, N.N., *BCL-2 family proteins: critical checkpoints of apoptotic cell death.* Clin Cancer Res, 2007. **13**(24): p. 7254-63.
56. Guicciardi, M.E. and G.J. Gores, *Life and death by death receptors.* FASEB J, 2009. **23**(6): p. 1625-37.
57. Salvesen, G.S. and V.M. Dixit, *Caspase activation: the induced-proximity model.* Proc Natl Acad Sci U S A, 1999. **96**(20): p. 10964-7.
58. Fulda, S., *Targeting extrinsic apoptosis in cancer: Challenges and opportunities.* Semin Cell Dev Biol, 2015. **39**: p. 20-5.
59. Degterev, A., M. Boyce, and J. Yuan, *A decade of caspases.* Oncogene, 2003. **22**(53): p. 8543-67.
60. Wang, J., et al., *A reproducible brain tumour model established from human glioblastoma biopsies.* BMC Cancer, 2009. **9**: p. 465.
61. Hossain, J.A., et al., *Long-term treatment with valganciclovir improves lentiviral suicide gene therapy of glioblastoma.* Neuro Oncol, 2019. **21**(7): p. 890-900.
62. Martinez-Murillo, R. and A. Martinez, *Standardization of an orthotopic mouse brain tumor model following transplantation of CT-2A astrocytoma cells.* Histol Histopathol, 2007. **22**(12): p. 1309-26.

63. Szatmari, T., et al., *Detailed characterization of the mouse glioma 261 tumor model for experimental glioblastoma therapy.* Cancer Sci, 2006. **97**(6): p. 546-53.
64. Abcam. *Counting cells using a hemocytometer*. Available from: https://www.abcam.com/protocols/counting-cells-using-a-haemocytometer.
65. Invitrogen. *NuPAGE Technical Guide: General information and protocols for using the NuPAGE electrophoresis system*. 2003; Available from: https://studylib.net/doc/8259348/nupage-technical-guide.
66. Krohne, T.U., et al., *Mechanisms of cell death induced by suicide genes encoding purine nucleoside phosphorylase and thymidine kinase in human hepatocellular carcinoma cells in vitro.* Hepatology, 2001. **34**(3): p. 511-8.
67. Heimer, S., et al., *Raptinal bypasses BAX, BAK, and BOK for mitochondrial outer membrane permeabilization and intrinsic apoptosis.* Cell Death Dis, 2019. **10**(8): p. 556.
68. Hossain, J.A., et al., *Suicide gene therapy for the treatment of high-grade glioma: past lessons, present trends, and future prospects.* Neurooncol Adv, 2020. **2**(1): p. vdaa013.
69. Melcher, A., et al., *Tumor immunogenicity is determined by the mechanism of cell death via induction of heat shock protein expression.* Nat Med, 1998. **4**(5): p. 581-7.
70. Podergajs, N., et al., *Expansive growth of two glioblastoma stem-like cell lines is mediated by bFGF and not by EGF.* Radiol Oncol, 2013. **47**(4): p. 330-7.
71. Glaser, T., et al., *Death receptor-independent cytochrome c release and caspase activation mediate thymidine kinase plus ganciclovir-mediated cytotoxicity in LN-18 and LN-229 human malignant glioma cells.* Gene Ther, 2001. **8**(6): p. 469-76.
72. Seitz, S.J., et al., *Chemotherapy-induced apoptosis in hepatocellular carcinoma involves the p53 family and is mediated via the extrinsic and the intrinsic pathway.* Int J Cancer, 2010. **126**(9): p. 2049-66.
73. Roy, S. and D.W. Nicholson, *Cross-talk in cell death signaling.* J Exp Med, 2000. **192**(8): p. F21-5.
74. Tomicic, M.T., R. Thust, and B. Kaina, *Ganciclovir-induced apoptosis in HSV-1 thymidine kinase expressing cells: critical role of DNA breaks, Bcl-2 decline and caspase-9 activation.* Oncogene, 2002. **21**(14): p. 2141-53.
75. Vigneswara, V. and Z. Ahmed, *The Role of Caspase-2 in Regulating Cell Fate.* Cells, 2020. **9**(5).

76. Dong, F., S. Soubeyrand, and R.J. Hache, *Activation of PARP-1 in response to bleomycin depends on the Ku antigen and protein phosphatase 5.* Oncogene, 2010. **29**(14): p. 2093-103.

77. Chen, A., *PARP inhibitors: its role in treatment of cancer.* Chin J Cancer, 2011. **30**(7): p. 463-71.

78. Peralta-Leal, A., M.I. Rodriguez, and F.J. Oliver, *Poly(ADP-ribose)polymerase-1 (PARP-1) in carcinogenesis: potential role of PARP inhibitors in cancer treatment.* Clin Transl Oncol, 2008. **10**(6): p. 318-23.

79. Prietsch, R.F., et al., *Genistein induces apoptosis and autophagy in human breast MCF-7 cells by modulating the expression of proapoptotic factors and oxidative stress enzymes.* Mol Cell Biochem, 2014. **390**(1-2): p. 235-42.

80. Lin, C.Y., et al., *Simultaneous induction of apoptosis and necroptosis by Tanshinone IIA in human hepatocellular carcinoma HepG2 cells.* Cell Death Discov, 2016. **2**: p. 16065.